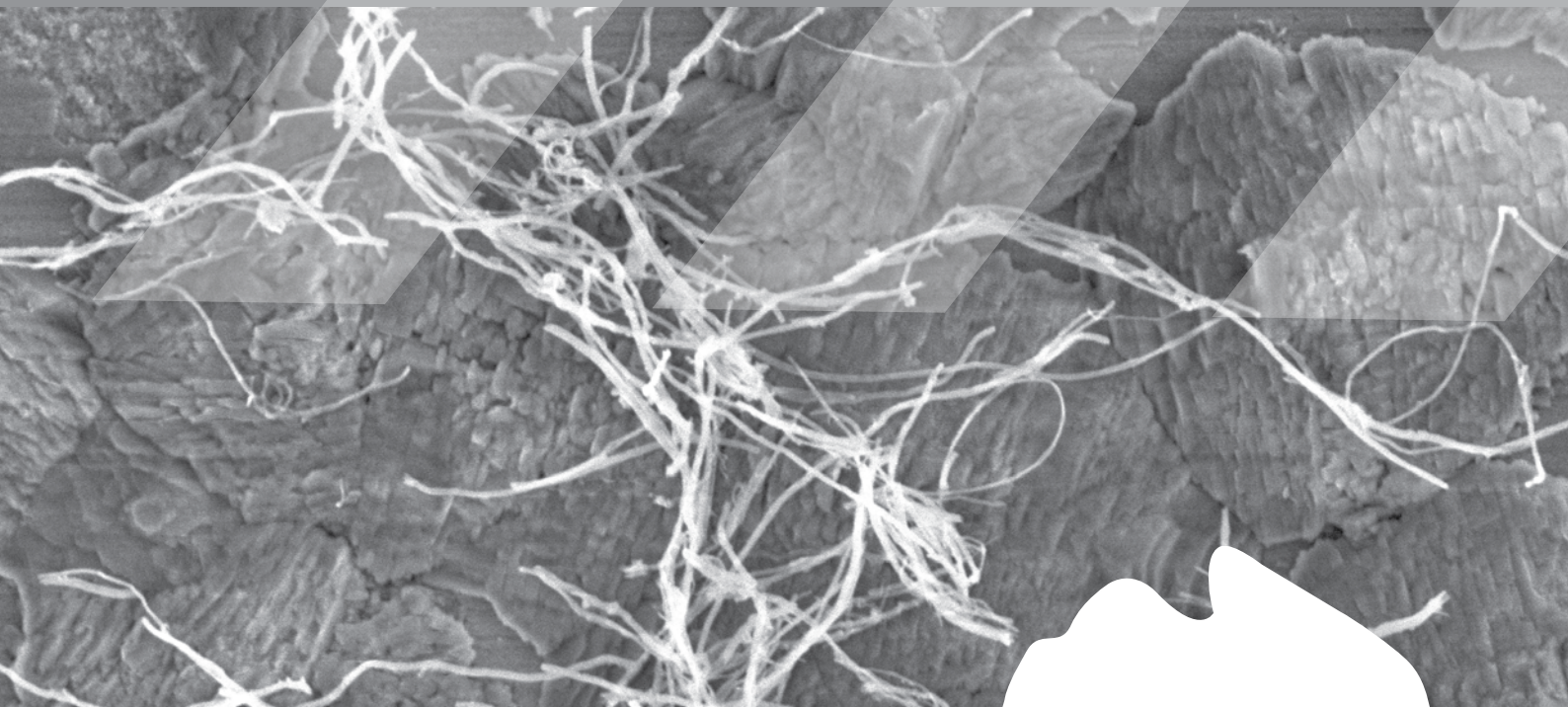




safe work australia

Developing Workplace Detection and Measurement Techniques for Carbon Nanotubes



June 2010



Developing Workplace Detection and Measurement Techniques for Carbon Nanotubes

Acknowledgement

This report was produced by CSIRO under commission from Safe Work Australia, through funding provided under the National Nanotechnology Strategy. The report was written by Dr Jurg Schutz, Dr Brendan Halliburton and Dr Stephen Brown with assistance from Dr Robert White, Dr David Evans, Luke Grundy, Chris Coombs, Dr Kallista Sears, Chi Huynh and Dr Stephen Hawkins.

The authors wish to thank Safe Work Australia's Nanotechnology OHS Advisory Group and the Nanotechnology OHS Measurement Reference Group for reviewing the report and gratefully acknowledge comments received on the report from Garry Gately (Australian Institute of Occupational Hygienists), Dr Howard Morris (Safe Work Australia) and Professor Lidia Morawska (Queensland University of Technology).

The construction of purpose-built test equipment and execution of associated experiments were funded by the CSIRO Future Manufacturing Flagship. Sophisticated air sampling equipment was provided by CSIRO Energy Technology, carbon nanotubes were supplied by CSIRO Materials Science and Engineering and computing infrastructure of CSIRO Minerals was used for fluid dynamics modelling.

Disclaimer

The information provided in this document is based on scientific experiments under controlled laboratory conditions and can only assist you in the most general way. This document does not replace, or describe requirements for compliance with, any statutory requirements under any relevant State and Territory legislation. Safe Work Australia and CSIRO are not liable for any loss resulting from any action taken or reliance made by you on the information or material contained on this document. Before relying on the material, users should carefully make their own assessment as to its accuracy, currency, completeness and relevance for their purposes, and should obtain any appropriate professional advice relevant to their particular circumstances.

To the extent that the material on this document includes views or recommendations of third parties, such views or recommendations do not necessarily reflect the views of Safe Work Australia or CSIRO or indicate their commitment to a particular course of action.



Copyright Notice

© Commonwealth of Australia 2010

ISBN 978-0-642-33086-4 (Online PDF)

ISBN 978-0-642-33087-1 (Online RTF)

This work is copyright. You may download, display, print and reproduce this material for your personal, non-commercial use within your organisation, provided that an appropriate acknowledgement is made (retaining this notice), and the material is not altered or subjected to derogatory treatment. Apart from any use as permitted under the Copyright Act 1968, all other rights are reserved. Requests and inquiries concerning reproduction and rights should be addressed to:

Commonwealth Copyright Administration

Attorney-General's Department

3 – 5 National Circuit

Barton ACT 2600

Email: commonwealth.copyright@ag.gov.au

Web: <http://www.ag.gov.au/cca>

Executive Summary

The pathways through which carbon nanotubes (CNT) can enter the human body are currently the subject of intensive studies nationally and internationally, as are investigations for determining levels of exposure in the workplace and developing guidelines for the safe use of nanomaterials in the workplace.

This report investigates possible approaches for detecting nano-objects that are formed from airborne carbon nanotubes (CNT), while placing special emphasis on the very fine multi-wall carbon nanotubes (MWCNT) that are used for the manufacture of optically transparent CNT sheet electrodes or CNT yarns.

The OECD Working Party on Manufactured Nanomaterials (WPMN) has developed guidance on the initial assessment of emissions from nanomaterial processing, which is based on the use of hand-held sampling instruments in combination with membrane sampling. This approach has been used successfully by Johnson et al. [34] to evaluate emissions from water suspensions of various carbon-based nanomaterials (including fine CNT of 10-20 nanometres [nm] diameter) from laboratory processes.

Similar techniques were used as part of initial investigations in CSIRO's Belmont Laboratories to investigate emissions from the CNT yarn spinning process, but no CNT were detected. This led researchers to question:

1. Are there no CNT emitted as aerosols? or
2. Are there problems with the methodology used in detecting emissions of the very fine, spinnable CNT?

Thus a more detailed investigation was undertaken that involved the use of a Scanning Mobility Particle Sizer (SMPS) and an Electrostatic Low-Pressure Impactor (ELPI) – but again, no CNT were detected. The uncertainty in relation to questions 1 and 2 above had not been resolved.

To check the sensing potential of the methodology, a hermetically sealed test duct was built that allowed safe handling of hazardous aerosols. Results from the use of ELPI and SMPS to examine CNT aerosols showed clearly that airborne fine, spinnable CNT can be detected by these instruments in real-time and that CNT structures from only a few CNT to larger constructs are collected on the ELPI impactor plates.

Thus, there may be potential to use an ELPI for further investigations in workplace settings. Possibly, it could be used for confirmation where no material is detected using the OECD WPMN initial assessment guidance [17]. It has the advantage of being able to capture aerosol particles from large volumes of air and form a concentrated deposit over a small area.

This report provides more detailed information on CSIRO's investigations, which were conducted on two levels:

- **Measure potential nanoparticle release in a CNT yarn production facility:** Air samples were taken from the vicinity of a spinning device where CNT forests on a wafer are turned into CNT yarns under the influence of a twisting action at high rotational speed and analysed.
- **Evaluate the sensitivity of nanoparticle detection methods:** CNT-specific responses for CNT aerosols were measured using a variety of sampling procedures and sampling instrumentation under exclusion of natural background particles.

Sampling cassettes containing gold-coated polycarbonate membranes and equipped with conductive cowls of 25 mm diameter were evaluated as one of the potential detection methods. These devices are widely used by occupational hygienists for detecting asbestos fibres. A modified version of the sampling technique described in the Scanning Electron Microscopy (SEM) Method of ISO Standard 14966 was followed in the experiments of this report.

Investigations conducted in the CNT yarn production facility have so far not identified any CNT in the air and it is not currently known if the spinning of CNT yarns in fact produces loose airborne CNT. However, in the absence of any CNT objects identified it is still possible to determine an upper limit for the concentration of airborne CNT in the air. Results of this study suggest that concentration monitoring of fine CNT (i.e. CNT of 10nm diameter) by means of ISO 14966 may, for practical reasons, be difficult at concentrations below approximately one fibre per millilitre (fibre/ml) of air.

From the investigation of spinnable CNT deposits on these membranes by means of SEM it was further possible to establish that each CNT fibre had on average been broken into 50 pieces. This result is attributed to the influence of shear forces from an ultrasonic bath that was used for dispersing the CNT in a compatible solvent. This observation of high-level breakage may be specific to very high-aspect ratio CNT as other CNT were not investigated.

The air in the CNT yarn production facility was also analysed by commercial nanoparticle sampling instrumentation, which included a Scanning Mobility Particle Sizer (SMPS) and an Electrostatic Low-Pressure Impactor (ELPI) amongst other portable equipment capable of detecting nanoparticles. None of the instruments registered significant changes in measured particle concentration or particle number distribution that could be attributed to the operation of the CNT yarn spinning device.

However, since fine MWCNT are very hard to detect against the naturally occurring nanoparticle background of a manufacturing site or a laboratory, further investigations were conducted to evaluate the above nanoparticle sampling techniques against a challenge of synthetically generated CNT-objects under the exclusion of background particles in a sealed containment. Via this approach it is possible to obtain CNT specific responses from these instruments. Measurements conducted using the SMPS or the ELPI show clearly that CNT aerosol can be generated in large concentrations by nebulising CNT dispersions. This was demonstrated for spinnable MWCNT of 10nm diameter as well as for coarser MWCNT from a different growth process with diameters ranging from 50nm to 100nm. SEM images of MWCNT objects collected by the ELPI

provide evidence of significant differences between the morphologies of agglomerates formed by the fine and the coarse MWCNT.

The aerosol characterisation work was undertaken in the test duct at very high concentrations of CNT in nitrogen ($5 \cdot 10^5$ structures per cm^3), with limited background contamination and variation in background particle levels. Experimental considerations for membrane sampling include membrane type, cowl orientation, membrane coating, and membrane pore size. Further work is needed to determine whether these methods would be successful at detecting fine CNT in workplace settings at low concentrations and with varying background levels.

- The ELPI has the capacity to capture aerosol particles from large volumes of air and form a concentrated deposit of captured particles over a small area. This ability is valuable because it addresses the shortcomings of membranes, where limitations on sampling rate (via the pore size required to capture nanoparticles) and sampling time (via eight hour working days) determine the volume of sampled air that can be processed. It also allows imaging of particles after collection to determine if fibrous structures of concern are present.
- Background-free test aerosols can also be useful for assessing in detail the sensitivity of membrane-based sampling for aerosols of nanoparticles other than carbon nanotubes. This includes measurements that specify the minimum requirement for membrane pore size that ensures particles are not lost.



Contents

| | | |
|----------|--|-----------|
| 1 | Project Overview | 6 |
| 2 | Known Methods for Assessing CNT Emissions and Exposure | 8 |
| 3 | Methods Used by CSIRO | 10 |
| 3.1 | Carbon nanotube materials | 10 |
| 3.2 | The CNT emissions process at the centre of this study | 12 |
| 3.3 | Membrane-based air sampling | 12 |
| 3.3.1 | Air sampling protocols | 13 |
| 3.3.2 | Analysis of membrane samples by electron microscopy | 14 |
| 3.4 | Object analysis by real-time particle sampling | 15 |
| 3.4.1 | Overview | 15 |
| 3.4.2 | Real-time particle measurement equipment | 15 |
| 3.5 | Synthetic carbon nanotube aerosols | 17 |
| 4 | Results 19 | |
| 4.1 | Application of common sampling techniques to detect potential CNT aerosols in the Carbon Nanotube Yarn Spinning Laboratory in Belmont, Geelong | 19 |
| 4.1.1 | Air sampling results | 20 |
| 4.1.2 | Real-time sampling results | 20 |
| 4.2 | Synthetic carbon nanotube aerosols | 22 |
| 4.2.1 | Initial evaluation of the test duct | 22 |
| 4.2.2 | CNT aerosol characterisation by SMPS | 23 |
| 4.2.3 | ELPI real-time measurements | 24 |
| 4.2.4 | ELPI particle number concentrations | 26 |
| 4.2.5 | Particle structure information from the ELPI | 27 |
| 4.2.6 | Membrane-based sampling of synthetic CNT objects | 32 |
| 5 | Discussion | 36 |
| 5.1 | Information from real-time data | 36 |
| 5.1.1 | CNT yarn spinning laboratory | 36 |
| 5.1.2 | SMPS measurements in test duct | 36 |
| 5.1.3 | ELPI measurements in test duct | 36 |
| 5.2 | Structure information for CNT objects from the ELPI | 37 |
| 5.3 | Membrane-based sampling | 38 |
| 5.3.1 | Analysis of air samples from CNT yarn spinning laboratory | 38 |
| 5.3.2 | Analysis of synthetic CNT objects | 38 |
| 5.4 | Implications of findings for detecting carbon nanotubes | 40 |
| 6 | Summary | 41 |
| 7 | Relation of this CNT Detection Work to Other Work and Approaches | 43 |
| 8 | Conclusions and Issues for Further Consideration | 44 |
| | References | 46 |
| | Appendix A: Background-“Free” Challenges of Synthetic Carbon Nanotubes | 50 |
| | Aerosol generation | 50 |
| | Containment for synthetic hazardous aerosols and sampling provisions | 50 |



Appendix B: Selection of Membranes54
Appendix C: Reference Membranes58
Appendix D: Analysis of Membrane Samples by Electron Microscopy62
Appendix E: Upper Detection Limits65
Appendix F: Assessment Of The Laboratory Air Environment67
Background 67
Results 67
Summary 69

List of Figures

| | |
|---|----|
| Figure 1: SEM images of Carbon Nanotube forests grown by the Catalyst Pre-Deposition method: Spinnable forest of 500µm long CNT (left) and CNT forest of short fibres of 2-3µm length (right)..... | 11 |
| Figure 2: High-resolution TEM images of Carbon Nanotubes grown by the Catalyst Pre-Deposition method..... | 11 |
| Figure 3: Image of the Hazardous Aerosol Test Duct showing the Cowl Chamber in the centre and on the right the SMPS attached to the second set of sampling tubes..... | 18 |
| Figure 4: Examples of fibrous structures found on the Mixed Cellulose Ester membrane using Phase Contrast Microscopy, after conversion of the membrane to an optically transparent gel..... | 19 |
| Figure 5: SEM image of the surface of track-etched Polycarbonate membranes (a gold-coated membrane with 100nm pores; refer to Appendix B:) after 87 minutes of air sampling at 2 LPM in the Belmont Yarn Spinning Laboratory..... | 21 |
| Figure 6: SMPS scans of 232nm PSL spheres dispersed in analytical grade 2-propanol. The concentration of PSL spheres in solution was lower for Scans 1 and 2 in comparison to Scans 3 to 5..... | 22 |
| Figure 7: A series of SMPS scans (see Section 3.4.2 for instrument details) from spinnable CNT dispersed in 2-propanol ("CNT + 2-propanol"), the 2-propanol on its own ("2-propanol") and for an ultra-high purity 2-propanol ("UHP Grade 2-propanol")..... | 23 |
| Figure 8: SMPS particle distribution of spinnable carbon nanotubes when nebulised from 2-propanol..... | 24 |
| Figure 9: ELPI time series of total electrometer current for spinnable carbon nanotubes, the 2-propanol solvent as well as for high purity 2-propanol..... | 25 |
| Figure 10: ELPI particle distribution of spinnable CNT when nebulised from 2-propanol..... | 26 |
| Figure 11: Optical image of spinnable CNT objects collected on ELPI impactor plate 13. Enlarged views of objects in yellow and red circle are shown in Figure 12..... | 27 |
| Figure 12: Enlarged optical images of spinnable CNT objects collected on ELPI impactor plate 13 from Figure 11 (400x magnification). The object from the yellow (red) circle is shown on the left (right) side..... | 28 |
| Figure 13: Optical image of spinnable CNT objects collected (marked by arrows) on the circlip of ELPI impactor plate 10 (~40x magnification). The aluminium foil substrate can be seen towards the left side of the image..... | 29 |
| Figure 14: SEM images of CCI CNT (left) and Spinnable CNT (right) collected on ELPI impactor plates 1 to 4 (all at the same magnification)..... | 30 |
| Figure 15: SEM images of CCI CNT of large size (left) and an illustration of the size range observed for Spinnable CNT at high magnification (right)..... | 31 |
| Figure 16: Optical images of CNT objects deposited on the polycarbonate membrane from an airstream sampled through a 3/8" sampling tube (10x magnification)..... | 33 |
| Figure 17: A series of optical images taken to highlight the detailed structure of the CNT object..... | 34 |
| Figure 18: Optical microscope images of CNT objects found on gold-coated membrane surfaces from sampling of CNT aerosols by the cowl of the <i>Test Duct</i> . Images on the left (right) show membrane surfaces where the cowl had been pointing downwards (upwards). Scale bars in millimetres are provided on the right border: the magnification in the upper row was 4x and 50x in the bottom row..... | 35 |

| | | |
|------------|--|----|
| Figure 19: | Design sketch of the Hazardous Aerosol Test Duct..... | 51 |
| Figure 20: | Simulation of airflow streamlines inside the 199 mm cylindrical section of the cowl. The airflow at the inlet is 150 standard litres per minute (SLPM). From this flow 2 SLPM are drawn through the sampling cowl on top of the Cowl Chamber, while the remaining flow is exiting the unit through the outlet behind the HEPA filter..... | 52 |
| Figure 21: | Likely path of dust particles passing through the Cowl Chamber and landing on the membrane inside the cowl for inlet flow rates of 10 SLPM (left) and 150 SLPM (right).52 | |
| Figure 22: | SEM image of a tortuous-path Silver Membrane with 0.45µm nominal pore size (left) and of a track-etched Polycarbonate membrane with straight cylindrical pores of 200nm diameter (right) at comparable scales. | 54 |
| Figure 23: | Schematic diagrams of tests used for assessing membrane permeance. <i>Top:</i> Closed system set up (left) where the membrane under test is exposed to a pressure differential and the change of pressure on the permeate side is monitored over time (right). <i>Bottom:</i> System where a constant flow is maintained through the membrane (in the membrane holder) by a piston vacuum pump / mass flow controller (MFC) combination. Permeance is characterised by the pressure that is built up across the membrane at the given flow. | 55 |
| Figure 24: | Pressure differential required across polycarbonate membranes of different pore sizes (see legend) to obtain a certain mass flow rate. These values apply for an Aalborg MFC of 5 litres per minute maximum flow. | 56 |
| Figure 25: | Identification of the inorganic nature of a coarse fibrous fragment by Energy Dispersive X-Ray Spectroscopy (EDXS). | 57 |
| Figure 26: | Spinnable Carbon Nanotubes applied to gold-coated polycarbonate membranes with 100nm pore size from a 2-propanol dispersion. SEM magnification is increased from top to bottom (indicated in the top left corner), while the nominal application level (i.e. assuming all CNT are 200 µm long) is increased between columns: 7,000 fibres/mm ² (left), 70,000 fibres/mm ² (centre) and 350,000 fibres/mm ² (right)..... | 59 |
| Figure 27: | Spinnable Carbon Nanotubes applied to gold-coated polycarbonate membranes with 100nm pore size from a 2-propanol dispersion. Nominal fibre concentrations are indicated on the right. The location of the single spinnable CNT that was found in the upper 2 images is marked by arrows. The fibre in the image at the bottom exceeds the diameter of spinnable CNT. | 60 |
| Figure 28: | SEM image of frame _005 from Table 5 with a hand-drawn sketch that was used to apply the counting rules (inset). | 63 |
| Figure 29: | Wind pattern in the vicinity of Belmont (Grovedale) on day of sampling. | 69 |
| Figure 30: | Aerotrak (A) sampling at the spinning process (interruption of time process noted in the plot). | 69 |

List of Tables

| | | |
|----------|---|----|
| Table 1: | Comparison of sampling techniques used in conjunction with Asbestos to determine fibre concentrations..... | 9 |
| Table 2: | Properties of CSIRO-grown Carbon Nanotubes | 10 |
| Table 3: | Comparison of permeances of polycarbonate membranes in uncoated condition “As is” and after application of a gold coating of 80nm thickness..... | 55 |
| Table 4: | Comparison of flow rates set by the Mass Flow Controller (column MFC) to calculated flow rates based on pressure differential and membrane permeances. | 56 |

| | |
|---|----|
| Table 5: Summary of objects counted on 13 randomly selected view fields from a gold-coated polycarbonate membrane of 100nm pore size with a nominal CNT fibre density of 7000 fibres/mm ² (see Section 3.3.1 for preparation details)..... | 64 |
| Table 6: Aerosol sampling results (average concentrations) | 68 |

Abbreviations

| | |
|-------|--|
| CCI | Continuous Catalyst Injection (also Catalyst Co-Injection) |
| CNT | Carbon Nanotube(s) |
| CPC | Condensation Particle Counter |
| CVD | Chemical Vapour Deposition |
| DL | Detection Limit |
| EDXS | Energy Dispersive X-ray Spectroscopy |
| ELPI | Electrostatic Low-Pressure Impactor |
| HEPA | High Efficiency Particulate Air (filter) |
| LPM | Litres per minute |
| MCE | Mixed Cellulose Ester (membrane) |
| MFC | Mass Flow Controller |
| MWCNT | Multi-Wall Carbon Nanotube(s) |
| OECD | Organisation for Economic Co-operation and Development |
| OPC | Optical Particle Counter |
| PC | PolyCarbonate (membrane) |
| PCM | Phase-Contrast Microscopy |
| PSL | Polystyrene Latex |
| SEM | Scanning Electron Microscopy |
| SLPM | Standard Litres Per Minute |
| SMPS | Scanning Mobility Particle Sizer |
| SPM | Scanning Probe Microscopy |
| SWCNT | Single-Wall Carbon Nanotube(s) |
| TEM | Transmission Electron Microscopy |

1 Project Overview

Aerosols containing airborne carbon nanotubes (CNT) are considered potentially more hazardous than general ultrafine or fine particle aerosols if inhaled, because they may exhibit fibre-related toxicities in addition to particle effects. This position is supported by recent toxicological studies, which suggest that the presence of CNT in the mesothelial layer of the chest or abdomen can stimulate the release of mediators to an extent that causes a severe inflammatory response in the associated tissue [1], [2]. Another study [3] has shown that CNT can penetrate the membrane of lysosomes to reach the interior and from there cross the nuclear membrane of the cell.

This work is part of an initiative within CSIRO that is concerned with ensuring a safe approach to the manufacture of materials that are made of or contain nano-structured materials. At the core of this investigation is the potential for nano-structured materials (specifically carbon nanotubes) to become airborne during processing, and how best to detect them so that the effectiveness of measures taken for their control and containment can be verified.

New aspects investigated in this work concern the application of existing instrumentation and sampling technologies to detect CNT of 10nm diameter with length-to-diameter aspect ratios as high as 40,000. Common techniques are applicable to this scenario with some modification, as we will show in the experimental section of this report.

Membrane-based sampling techniques and real-time sampling instrumentation are investigated to determine how they can be applied to detecting CNT in a laboratory environment where materials containing CNT are processed. A CNT-specific Detection Limit (DL) is determined for the CNT Yarn Spinning Laboratory in Belmont by means of membrane sampling that is based on the SEM Method described in ISO Standard 14966:2002E [4], with some modifications that take account of specific properties of fine CNT (Appendix D). Means for reducing the DL to more appropriate levels are discussed and presented together with some reflections on the limitations of the technique.

Air sampling experiments conducted on 25 and 26 February 2009 in the CNT Yarn Spinning Laboratory involved the use of size-selective real-time (and semi-real-time) sampling equipment for fine and ultrafine particles, in addition to membrane-based sampling and portable air sampling equipment with intrinsic size selectivity (Model AM510 Laser Spectrometer "SidePak", Condensation Particle Counter "P-Track" Models 8525 or 3007, Nanoparticle Aerosol Monitor "AeroTrack 9000" from TSI Inc., USA). Size-resolving real-time sampling instruments comprised a Scanning Mobility Particle Sizer (SMPS) and an Electrostatic Low Pressure Impactor (ELPI). Both instruments count particles selectively by size, but apply different principles to achieve this and hence exploit particle properties in different ways.

The uncertainty attached to the hazard potential of CNT requires that number concentrations of these fibrous objects are determined separately from other particles so that an object-specific assessment can be applied. An important property that needs

to be determined for a fibre with large length-to-width aspect ratio is the equivalent of a spherical aerodynamic diameter. This cannot be done on the basis of fibre diameter and length alone because the geometrical morphology can strongly deviate from that of a straight fibre, e.g. by forming bundles with other objects or by forming coils. A hermetically sealed containment was used in a separate investigation reported here, where CNT aerosols could be generated safely and be analysed under exclusion of naturally occurring particle background.

2 Known Methods for Assessing CNT Emissions and Exposure

The pathways through which CNT can enter the human body are currently the subject of intensive studies nationally and internationally [5], as are investigations to determine levels of exposure in the workplace ([6],[7],[8],[9],[10],[11],[12]). Several monitoring standards are currently at our disposal for determining exposure levels to inorganic fibrous materials specifically targeting asbestos ([4], [13], [14], [15], [16]) and recent guidelines describe how to apply these to assessments in the workplace ([17],[18],[19],[20],[21]). The standards may be applied to fine multi-wall carbon nanotubes (MWCNT) with some modifications. In terms of real-time particle measurement it has been shown that equipment is now commercially available that has the capacity to detect nanoparticles of 2.5nm diameter [22]. Exposure monitoring studies conducted in the United States of America at the University of Dayton Research Institute by the National Institute of Occupational Safety and Health (NIOSH) [7] and in Korea [9] have used common real-time monitoring equipment for estimating the concentration of MWCNT in the vicinity of various production and processing sites. Diameter distributions of MWCNT used in these instances were quite broad within a typical size range of 60nm to 150nm. One group of researchers at the Massachusetts Institute of Technology (MIT) conducted pertinent measurements for much finer single-wall carbon nanotubes (SWCNT) at the exhaust of their reactor [12]. Fibrous nanofibre structures of 10-20nm diameter, which were not CNT, have been found in dusts generated from processing advanced composite structures that contained CNT [11].

Membrane-based collection of dust samples is widely used by hygienists for determining airborne fibre concentrations of asbestos in workplaces. A summary of pertinent standards is shown in Table 1. Note that this list represents only a selection of applicable standards and is by no means comprehensive.

These techniques are used in conjunction with a small range of asbestos-specific counting rules that differ slightly between different standards. It is generally necessary to adapt counting rules to suit specific properties of the target fibre species including size and morphology. Once these rules have been established, it is essential that they are applied consistently throughout an investigation.

The simplest method of all the techniques listed in Table 1 involves the use of silver membranes in conjunction with SEM [23]. The most complex methods are those aiming to use TEM for the dust analysis. Within the latter group of methods are two subgroups that use different types of membranes for the collection of dust particles. Mixed cellulose ester (MCE) membranes have a sponge-like structure and their pores are tortuous. Polycarbonate (PC) membranes on the other hand have a flat surface and straight cylindrical pores (tortuosity ≈ 1 ¹). In both cases it is necessary to chemically dissolve the membranes at the end of the preparation step (see Table 1), but MCE membranes require an application of additional steps by which the sponge-like structure of the membrane is first collapsed into forming a film and subsequently subjected to plasma ashing. The plasma is needed to remove the surface of the

¹ Length of the pore divided by the membrane thickness.

membrane film to expose particulate structures located underneath so that they can be consolidated by the application of a carbon film for transfer of the structures to the TEM grid.

Table 1: Comparison of sampling techniques used in conjunction with asbestos to determine fibre concentrations

| METHOD | PCM | SEM | | TEM | |
|---|---|--------|----------------------------------|--|-----------------------------------|
| Standard(s) | ASTM D7201-06 NOHSC:3003 | | ISO 14966:2002E | ISO 10312:1995 ASTM D6281-06 NIOSH 7402 ² | |
| References | [13]; [14] | [23] | [4] | [15]; [16]; [24] | |
| Membrane | MCE | Silver | PC | PC | MCE |
| Pre-Treatment | - | - | gold coating | - | - |
| Sample Preparation | | | | | |
| A | conversion to optically transparent gel | - | plasma ashing to remove organics | apply carbon film | collapse membrane |
| B | | | | transfer to TEM grid | plasma ashing to expose particles |
| C | | | | dissolve membrane | apply carbon film |
| D | | | | | transfer to TEM grid |
| E | | | | | dissolve membrane |
| Microscopy | PCM (option: TEM) | SEM | SEM | TEM | TEM |
| Dust Deposit Range: (fibres/mm²) | ASTM: 100 to 1,300 | - | 3 to 200 | ISO:50 to 7000 ASTM: < 7,000 NIOSH: 100 to 1,300 | |
| Measuring Limit ³: (fibres/m³) | ASTM: ≈ 40,000 NOHSC: <10,000 | - | 100 (L>5µm) to 300 | ISO: 500 ASTM: no lower limit NIOSH: ≈ 40,000 | |

Abbreviations

Membranes: MCE: Mixed Cellulose Ester; PC: Track-Etched Polycarbonate
Microscopy: PCM: Phase Contrast Microscopy; SEM: Scanning Electron Microscopy; TEM: Transmission Electron Microscopy

² NIOSH 7402 discusses the use of MCE membranes that does not apply the plasma ashing.

³ Value is typically specified for a sampling volume of 1 m³.

3 Methods Used by CSIRO

In this report we describe the generation, sampling and imaging of airborne structures obtained from fairly fine MWCNT of 10nm diameter ([25],[26]) which are used for the manufacture of CNT yarns [27]. Various alternatives for detecting airborne nano-objects formed from fine CNT of 10nm diameter are evaluated. Comparisons are also made to coarser CNT from a different growth process, which have a broad range of diameters in the vicinity of 80nm.

The project consists of two main activities as follows:

- State-of-the-art aerosol sampling and analysis techniques are used to search for aerosols generated unintentionally in a laboratory environment where Carbon Nanotube (CNT) yarns are spun from specially grown “CNT forests” and to characterise particle fractions that potentially contain CNT by size, structure and concentration.
- State-of-the art aerosol sampling and analysis techniques evaluated at very low particle backgrounds on synthetic CNT aerosols generated by atomisation of CNT dispersions.

Nano-object detection and characterisation have been conducted by two different techniques, which provide characteristic information on different aspects of particles contained in the aerosol:

- The dust-laden airstream was sampled by collection on a membrane and nano-objects were later examined by microscopic means. This technique reveals size and structural information that is typical of objects collected from the air stream.
- Objects were also segregated into specific size fractions and counted in real time (or close to real time). Categorisation criteria differ between instruments and object counts are broken down into sizes according to these criteria.

Certain equipment in the latter group can also be used to collect objects for later analysis by microscopy. These are the Electrostatic Low-Pressure Impactor (ELPI) and the Nanoparticle Sampler.

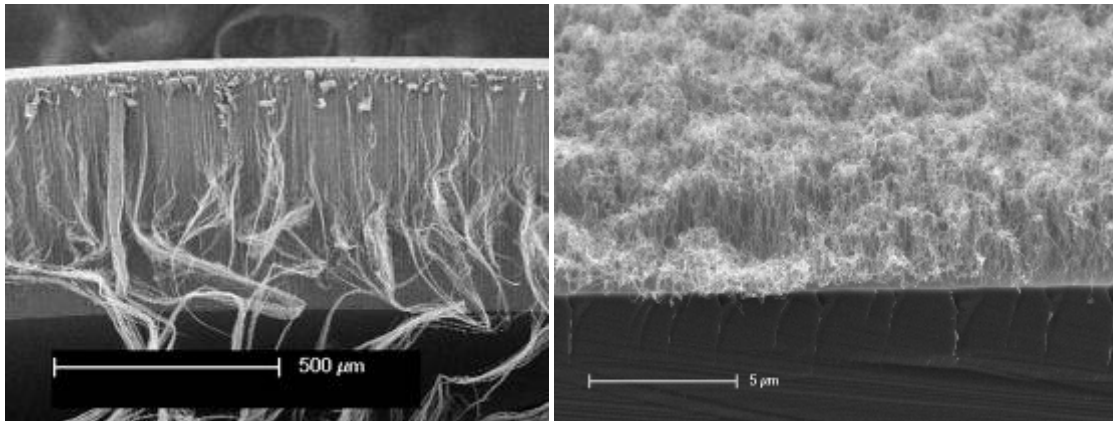
3.1 Carbon nanotube materials

Typical properties of CNT manufactured by CSIRO are summarised in Table 2. All CNT manufactured at CSIRO are grown by Chemical Vapour Deposition (CVD), but there are two different methods that are commonly used in conjunction with this technique.

Table 2: Properties of CSIRO-grown carbon nanotubes

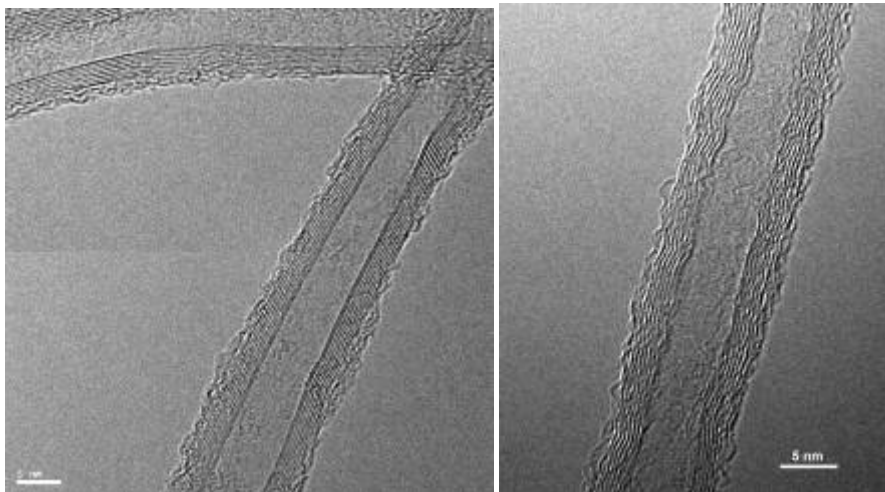
| Method | No. Walls | Diameter (nm) | Length (µm) | Aspect ratio | Catalyst Contamination | Branching |
|-----------|-----------|---------------|-------------|--------------|------------------------|--------------|
| Spinnable | 4 -10 | 9 – 20 | 3 – 600 | ≤ 40,000 | Low | V. Low - Med |
| CCI | ≥ 35 | 10 – 150 | 200 – 3000 | ≤ 40,000 | Med - High | Med - High |

In the first method, which is used for growing spinnable CNT ([28], [27]), an iron catalyst is deposited as a thin layer onto the surface of a silicon wafer substrate. This iron catalyst layer is broken up by the application of heat into a large number of nanoscale “islands”, which become the growth sites for the formation of CNT when the wafer is exposed to a suitable mix of process gases ([29], [30]). This method is often referred to as Catalyst Pre-Deposition (CPD) and delivers fine multi-walled CNT with very low levels of catalyst contamination (Figure 1 and Figure 2).



SEM by Chi Huynh (CSIRO)

Figure 1: SEM images of Carbon Nanotube forests grown by the Catalyst Pre-Deposition method: Spinnable forest of 500μm long CNT (left) and CNT forest of short fibres of 2-3μm length (right)



TEM by Kallista Sears and Chi Huynh (CSIRO), imaged at the Bio21 Institute in Melbourne

Figure 2: High-resolution TEM images of Carbon Nanotubes grown by the Catalyst Pre-Deposition method

In the second method, the iron catalyst is co-injected with the process gases into the reaction chamber where the silicon wafer growth substrate is located. This method is referred to as Continuous Catalyst Injection (CCI) and delivers a broad distribution of coarser CNT that contain significant levels of catalyst contamination. The production

volume of CCI is higher than that of CPD and therefore CCI is the preferred method for use in commercial applications such as reinforced composites.

3.2 The CNT emissions process at the centre of this study

The Carbon Nanotube Yarn Spinning Laboratory in Belmont, Geelong, was the main location where various air sampling techniques were tested for their suitability to detect and analyse Carbon Nanotube (CNT) aerosols.

In the manufacturing process investigated, CNT yarns are formed from specially grown “forests” of spinnable CNT, which have the capacity to release CNT in the form of a web structure. The web is drawn as a sheet from the forest and formed into a yarn by application of twist. It is considered that the CNT yarn spinning process might have the potential to release individual CNT or small bundles of CNT into the air, particularly at the point where the web-like CNT sheets are drawn from the forest. It is also known that CNT have an extremely high affinity to stick to each other or to other surfaces, which is due to van der Waals forces that are present on the fibre surfaces. These forces are predominantly responsible for holding the web together, which illustrates their strength. However, this is no guarantee that no CNT are being released into the air by the drawing process.

Personal protective equipment including a lab coat (polypropylene or cotton), normal safety glasses and a P2-rated respirator (half-face mask or disposable respirator) are worn in the laboratory where CNT yarns are manufactured. Protective equipment is not removed from the laboratory unless it is placed double-bagged into the hazardous waste disposal. Respirators are kept in sealed plastic bags when not in use.

In line with due diligence, we were aiming to measure concentration levels for airborne CNT in the laboratory or to determine a CNT-specific Detection Limit (DL) in the absence of any collected CNT.

To this end, CSIRO conducted air sampling investigations in Belmont by means of membrane-based sampling, supported by portable real-time sampling equipment such as the Laser Photometers and Condensation Particle Counters (CPC). The most extensive investigation which provided the data for this report involved additional real-time (and semi-real-time) sampling equipment including an Electrostatic Low-Pressure Impactor (ELPI), a Scanning Mobility Particle Sizer (SMPS) capable of detecting aerodynamic particle sizes down to about 10nm and an AeroTrack 9000 Nanoparticle Aerosol Monitor. These investigations are described in more detail in the following sections of the report.

3.3 Membrane-based air sampling

Membrane-based air sampling techniques are investigated in this section of the report to determine how they can be applied to detecting CNT in a laboratory environment where materials containing CNT are processed. A CNT-specific Detection Limit (DL) is determined for the CNT Yarn Spinning Laboratory in Belmont by means of membrane sampling that is based on the SEM Method described in ISO Standard 14966:2002E

[4], but includes a number of modifications required to account for specific properties of fine, spinnable CNT. Means for reducing the DL to more appropriate levels are discussed and presented together with some reflections on the limitations of the technique.

3.3.1 Air sampling protocols

Since none of the earlier air sampling investigations conducted at the CNT Yarn Spinning Laboratory in Belmont had produced evidence supporting the presence of aerosolized CNT in the air, the issue to understand is whether the process of spinning yarns from spinnable CNT forests either does not produce any airborne CNT or produces them at levels not detectable by the methodologies used. This scenario leads to the following questions:

- What would the surface of a membrane look like if it had been exposed to CNT aerosols of a certain concentration during sampling?
- What are the conditions under which we would be able to detect individual CNT (or small bundles of CNT) on a membrane after air sampling?

The first question was addressed by creating reference membranes with calculated number concentrations of deposited CNT, assuming that they had been sampled from a certain volume of air drawn through the membrane. For this, the CNT were dispersed in 2-propanol and applied by drawing the dispersion through the membrane using a fritted funnel as a support (Appendix C:).

From an imaging point of view it is possible to count individual fibres if the fibre density on the surface of the membrane is between 70 fibres/mm² and 7000 fibres/mm² (independent of the sampling volume), which corresponds to a fibre concentration in a range between 1 and 10 fibres/ml for a sampling volume of 300 litres of air. The upper limit of 7000 fibres/mm² is required to ensure that fibre ends are not obscured by other fibres. It is relatively high in comparison to recommendations made by various standards that have been developed for assessing asbestos fibres ([4], [13], [24]) but consistent with others ([15], [16]) – refer to Table 1. This is a result of the fineness of spinnable CNT, whose diameter of 10nm is distinctly lower than that of typical asbestos fibres. The lower limit provides for a reasonable probability that at least some fibres are found within 100 SEM frames.

We also found that a magnification of about 60,000x was required in order to see individual spinnable CNT fibres of 10nm diameter.

The second question concerns the conditions under which it is possible to conduct air sampling for (spinnable) CNT aerosols and analyse results by SEM. We assumed that polycarbonate membranes of 100nm pore size would be suitable for capturing the CNT objects. The membranes were coated with a relatively thick layer of gold that has no effect on the membrane permeance, but allows direct imaging by SEM without further treatment and provides a metallic substrate surface for Energy Dispersive X-Ray Spectroscopy (EDXS) that differs from the carbon signature of CNT.

From results summarised in Figure 24 we know that a maximum flow rate of four litres per minute can be reached for this type of membrane. However, it is advisable to avoid running the membrane at choke flow, so we have used a flow rate of two litres per minute. If sampling is conducted over a six hour day, we obtain a sampling volume of 720 litres. With a magnification of 60,000 that gives a viewing area of $16.5 \mu\text{m}^2$ and by counting CNT fibres in 100 frames, a sensitivity of 0.32 cm^{-3} is reached. ASTM Standard D 6620-06 [31] outlines how the sensitivity is calculated and how to obtain a Detection Limit (DL) for a power of choice (Appendix E). The power represents the probability for the correctness of the decision that sampled objects originate from the sampled air and not from the background of particles that were present on the membrane surface prior to sampling. We found in our experiments that the contamination level of gold-coated membranes was generally low enough to warrant setting the decision value to zero (Appendix E), but it would have been necessary to inspect a larger number of frames to establish this in accordance with the Standard. By assuming a decision value of zero, the Detection Limit for a power of 95% is 3.00 times the sensitivity, which is about 1 fibre/ml. The fibre density on the surface of the membrane is approximately 1800 fibres/mm^2 in this case, which lies in the recommended range of 70 to 7000 fibres/mm^2 .

3.3.2 Analysis of membrane samples by electron microscopy

The main steps in the analysis of membrane samples by electron microscopy, which can be either Scanning Electron Microscopy (SEM) or Transmission Electron Microscopy (TEM), generally include the following selections:

1. A suitable procedure to prepare the membrane samples for examination by electron microscopy.
2. An imaging method with a viewing range that is as large as possible, while giving the required resolution that individual fibres can be identified.
3. Adoption of counting rules that are appropriate for the main objects under investigation.

Asbestos standards (Table 1) provide an excellent description of the options available to address these points. It is however advisable to make minor adjustments since spinnable CNT are generally significantly thinner than asbestos fibres and consist of pure carbon. We applied at first some of the more common techniques to the problem (Section 4.1) and decided from experiences gained to use in this instance the SEM Method described in ISO Standard 14966:2002(E) [4] for our third series of experiments. We chose to give the SEM method preference over the TEM methods listed in Table 1 because the preparative steps prior to imaging were less onerous.

3.4 Object analysis by real-time particle sampling

3.4.1 Overview

Particle counting systems can provide total particle number concentrations as well as size dependent particle number distributions of an air sample. The propagation behaviour of a particulate object in an airstream depends on the material density of the particle, its morphology in terms of size and shape, electrostatic interactions with other charged surfaces and the dynamic interaction with the fluid stream. Different instruments tend to take these factors into account in different ways. While light scattering instruments provide mere number concentrations, other instruments include further 'in-flight' behaviour, such as aerodynamics in the case of the Electrostatic Low Pressure Impactor (ELPI) or electrostatic mobility in the case of the Scanning Mobility Particle Sizer (SMPS). The latter techniques have advantages for health related studies because the 'in-flight' aerodynamic behaviour is widely considered crucial for an accurate characterisation of how these particles penetrate into lungs during the breathing process. Additionally, the ELPI size selectively captures particles for subsequent physical and/or chemical analysis.

The following sections provide a more detailed description of the equipment, its use in conjunction with the Test Duct and a discussion of experimental results obtained from aerosols generated from dispersed CNT.

3.4.2 Real-time particle measurement equipment

Real-time sampling equipment available for experiments included a Scanning Mobility Particle Sizer (SMPS), an Electrostatic Low Pressure Impactor (ELPI) and a Nanoparticle Aerosol Monitor "AeroTrack 9000". All three instruments count particles selectively by size, but apply different principles to achieve this and hence exploit particle properties in different ways.

The SMPS can measure the spherical equivalent electrical mobility diameter of particles from approximately 2nm to approximately 1000nm with a resolution of greater than 64 particle "bins" or size cuts over this size range. This instrument is highly sensitive and can measure of the order of single particles per cm³ for any of the measured particle size bins. Particles from an air sample first pass through a pre-sizer that removes coarse particles before entering the instrument. The SMPS itself consists of two separate but coupled instruments, an Electrostatic Classifier (classifier) and a Condensation Particle Counter (CPC). By use of an electrostatic field, the classifier removes all particles from the air stream with the exception of those that fit into a narrow selected particle size bin. These size resolved particles exit the Classifier and are subsequently analysed by the CPC where particle numbers are resolved using laser beam counting techniques. However, to fully resolve particles over the entire size interval noted above two different SMPS systems are required:

- The 'nano' Electrostatic Classifier and 'nano' CPC use special sampling techniques to resolve particles with electrical mobility diameters less than approximately 10nm.

- For the larger particles the conventional Electrostatic Classifier is used and this instrument has a size range from approximately 10nm to 1000nm.

The larger diameter SMPS system was used for this study in order to have a better particle size bin overlap with the ELPI that allows comparisons to be made. The classifier used for the air sampling experiment was a Model 3071A (TSI Inc., USA) and the CPC used was a TSI Model 3775, which are both capable of reaching a response for particles down to about 10nm. The CPC was operated in low flow mode (0.3 SLPM) in conjunction with a custom built mass flow controller system for regulating and balancing the gas flow.

The ELPI uses the inertial properties of the particle to sequentially remove the larger diameter particles from the sample. However, prior to this sequential capture the particles are passed through a corona field charger where they acquire a saturation surface charge. When a particle is captured it releases this charge to one of the twelve sequential impactor stages, with this event registered by an electrometer connected to the respective stage as a charge current. The saturation charge of a particle is a fundamental property that depends primarily on the surface area of the particle. It can be determined experimentally and applied to the ELPI electrometer currents in the form of a calibration or scaling function to obtain respective number concentrations. Nano-objects such as carbon nanotubes deviate from the spherical model that is normally supplied by the manufacturer and used for this instrument and hence require the development of a CNT specific calibration function. The calibration function provided by the supplier was used exclusively in this report since the time frame of the project did not allow for a CNT specific calibration function to be determined.

The ELPI (from Dekati) operates at a flow rate of 10 LPM and provides 'real time' particle number concentration data with a sampling rate of 1Hz. It measures aerodynamic spherical equivalent diameter of particles within thirteen bins and has a size range extending from approximately 7nm to 10,000nm. This instrument has the capacity to also capture the counted particles on substrates for subsequent analysis by optical microscopy, SEM or TEM. Where larger quantities of the particles are available it is possible to weigh the substrates for gravimetric analysis.

However, under some conditions, particles can 'bounce' from one collecting plate to another with larger sized particles being deposited on a plate that would otherwise collect smaller particles. The degree of 'bounce' is dependent upon the 'stickiness' of the particle and the collection substrate. Generally a thin layer of grease is applied to the substrate to increase the adhesion of particles to the substrate and minimise particle bounce. In the intended design of the impactor, the calibration is insensitive to small deviations from the nominal position of the impactor plate and generally not affected by the grease layer.

The AeroTrack 9000 (from TSI) uses a diffusion charger to condition objects in the particle stream to assume a defined charge state in relation to surface area. It measures the transported charge from these objects and other operational parameters, which are subsequently processed into a single figure with unit $\mu\text{m}^2/\text{cm}^3$. The instrument has two response settings [32]:

- **Tracheobronchial (TB):** Characterise exposure for the coarser channels in human lungs; the highest adsorption capacity is attributed to particles with diameters in the vicinity of 3µm.
- **Alveolar (A):** Characterised exposure for the very fine pore tips in human lungs (alveoli); the highest adsorption capacity is attributed to particles with diameters of ca. 15 to 20µm.

3.5 Synthetic carbon nanotube aerosols

On-site air monitoring experiments conducted in the Carbon Nanotube (CNT) Yarn Spinning Laboratory prior to this investigation had delivered no evidence of aerosolised, spinnable CNT in the air of the laboratory. Since it is possible that no CNT are in fact aerosolised during the spinning process, it is necessary to find out more about the specific signatures of airborne CNT. This is best done in a gas stream that is free from naturally occurring nanoparticles in order to minimise interference. In the chosen approach, CNT aerosols are created in a test gas stream that is isolated from background particles for sampling by various membrane-based and real-time techniques capable of detecting such structures. These detection methods have been discussed in Section 3.4.2.

An instrument was constructed, the Hazardous Aerosol Test Duct (Figure 3), which can make these provisions by means of the following features:

- An atomiser for the generation of CNT aerosols.
- Sampling tubes for aerosol sampling by real-time detection techniques.
- A sampling cowl for membrane-based sampling.
- Various filter systems for safe use of the instrument where recirculation cannot be implemented.
- Absorber cartridges to strip solvent-vapours from the air stream and ensure reliable operation of the atomisation process.

Generation of synthetic CNT aerosols and provisions for a dust-free gas stream are discussed in Appendix A:. Results on the generation of CNT aerosols, the detection of CNT objects and their analysis are provided in Section 4.2.



Photo by Brendan Halliburton (CSIRO)

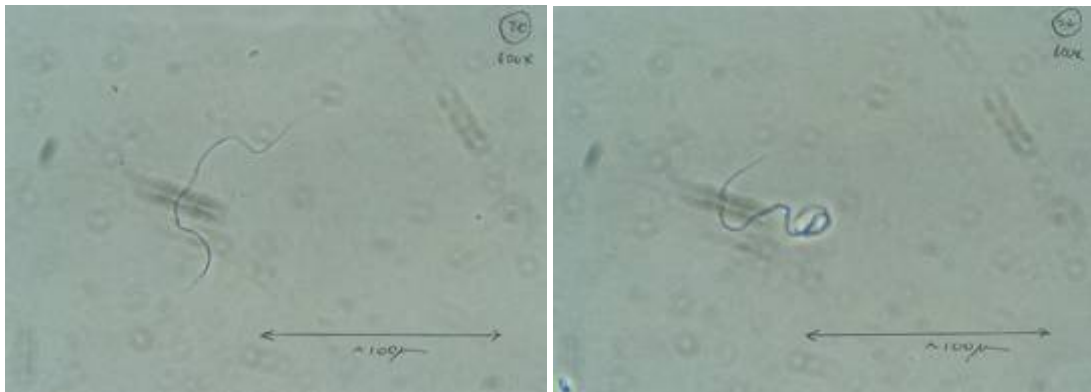
Figure 3: Image of the Hazardous Aerosol Test Duct showing the Cowl Chamber in the centre and on the right the SMPS attached to the second set of sampling tubes

4 Results

4.1 Application of common sampling techniques to detect potential CNT aerosols in the Carbon Nanotube Yarn Spinning Laboratory in Belmont, Geelong

Two investigations were conducted prior to work relating to this report and are briefly summarised in the following.

1. CSIRO commissioned Alert Solution (a Division of Bureau Veritas Australia Pty Limited) to apply the silver membrane technique [23] to the CNT yarn spinner in order to determine the extent to which the process released CNT into the air. The sampling was conducted at a flow rate of two litres per minute. The identification of fibrous structures by SEM with Energy Dispersive X-Ray Spectroscopy (EDXS) conducted in April and May 2007 on the rough membrane surface proved to be difficult and produced no evidence of airborne CNT.
2. The second sampling experiment was conducted in March 2008 where the potential of Phase Contrast Microscopy (PCM) method was investigated. The methodology was based on guidance from *Guidance Note On The Membrane Filter Method For Estimating Airborne Asbestos Fibres* [14]. Air in the vicinity of the CNT Yarn Spinner was drawn through a Mixed Cellulose Ester membrane of 0.8µm nominal pore size at a rate of 3-4 litres per minute. A number of fibrous structures with diameters ranging from 0.2 to 4 micrometres were found, some of which are shown in Figure 4. No CNT could be identified conclusively, particularly since the resolution of 200nm is not sufficient to detect individual CNT or small CNT bundles.



Photos by Steve Brown (CSIRO)

Figure 4: Examples of fibrous structures found on the Mixed Cellulose Ester membrane using Phase Contrast Microscopy, after conversion of the membrane to an optically transparent gel

3. The sampling experiments which form the basis for this report were conducted from the 25 to 26 February 2009, and involved a follow up measurement on 19 March 2009. The adopted methodology was similar to the SEM Method described in ISO Standard 14966:2002(E) [4], but was implemented with a number of modifications in

order to take into account the specific properties of CNT. These modifications are described in Appendices B to D and involved the following considerations:

- **Selection of Membranes** (Appendix B): the most appropriate selection of capillary pore membrane filters for the capture and analysis of aerosolised CNT:
 - Polycarbonate membranes with 100nm pore size, well below the recommended upper limit of 800nm [4] to reduce the risk of CNT fibres passing through the pores but large enough to allow an adequate gas flow through the membrane.
 - Use a deliberately thick gold coating around 80nm in thickness to mask the organic nature of the membrane.
- **Air Sampling Protocol** (Section 3.3.1, Appendix C): parameters for an air sampling protocol that reaches an adequate fibre-in-air detection limit for CNT sampling:
 - Adopt a target dust deposit range of 70 to 7000 fibres per mm².
 - Use a relatively low sampling rate that is suitable for the small membrane pore size (two litres per minute).
- **Analysis of Membrane Samples by Electron Microscopy** (Section 3.3.2, Appendix D): preparation of membranes and analysis of deposits on membranes by adapted counting rules:
 - Do not use plasma ashing because the treatment can destroy CNT.
 - Conduct SEM imaging at 60,000 magnification to resolve individual CNT.

4.1.1 Air sampling results

A typical SEM image of the membrane surface from a filter cassette after 87 minutes of sampling at 2 LPM in the CNT Yarn Spinning Laboratory on 26 February is shown in Figure 5. No CNT were captured.

4.1.2 Real-time sampling results

No significant change was observed that could clearly be attributed to the operation of the CNT yarn spinner, either from readings of the portable devices (SidePak, P-Track Model 8525, CPC Model 3007 and AeroTrack 9000) or from the particle size resolving instruments (SMPS, ELPI). Measurements obtained from portable devices used for assessing the laboratory and the outside atmosphere are provided in Appendix F. Results illustrate how a change in the wind direction can significantly change particle concentrations in the environment, which is followed with some delay by a pertinent change in the laboratory.

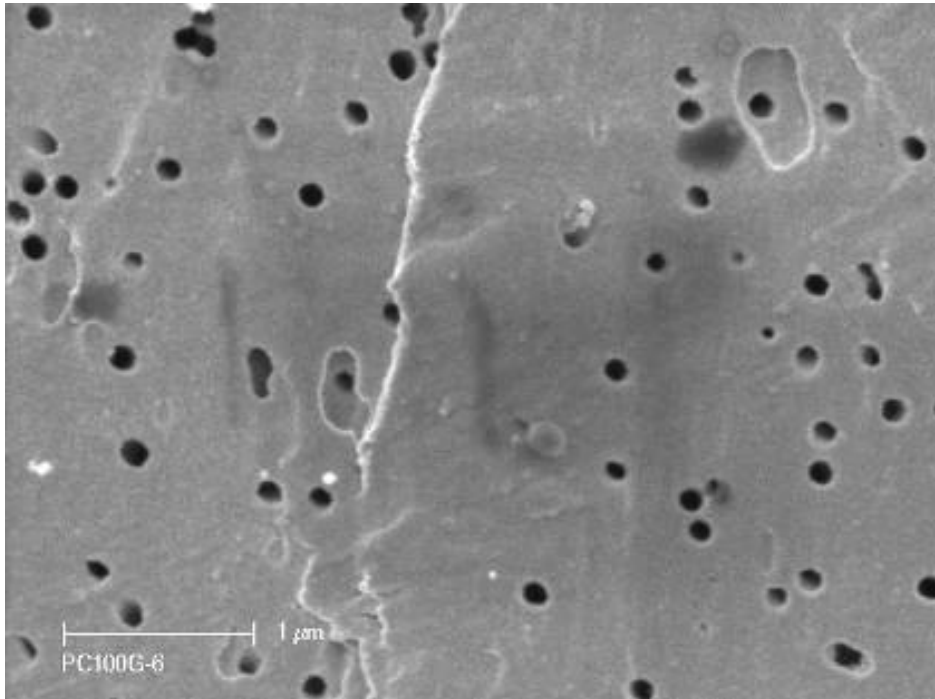


Figure 5: SEM image of the surface of track-etched Polycarbonate membranes (a gold-coated membrane with 100nm pores; refer to Appendix B:) after 87 minutes of air sampling at 2 LPM in the Belmont Yarn Spinning Laboratory

4.2 Synthetic carbon nanotube aerosols

Fine MWCNT are very hard to detect against the naturally occurring nanoparticle background of a manufacturing site or a laboratory. A hermetically sealed Test Duct that allows safe generation of synthetic CNT aerosols at low levels of particle background was used in this investigation (Appendix A) to verify the response of real time instruments and membrane-based sampling methods to CNT aerosol challenges. Through this approach it is possible to obtain CNT specific responses from pertinent nanoparticle sampling equipment and from nanoparticle monitoring techniques that are typically used for such applications.

4.2.1 Initial evaluation of the test duct

The first experiment that was conducted with the Test Duct for hazardous particle aerosols involved the atomisation of polystyrene latex (PSL) spheres of 232nm diameter in 2-propanol. The aerosol was sampled by the SMPS through one of the sampling tubes of the second set, which is located next to the cowl chamber. The result of five scans from the SMPS is shown in Figure 6.

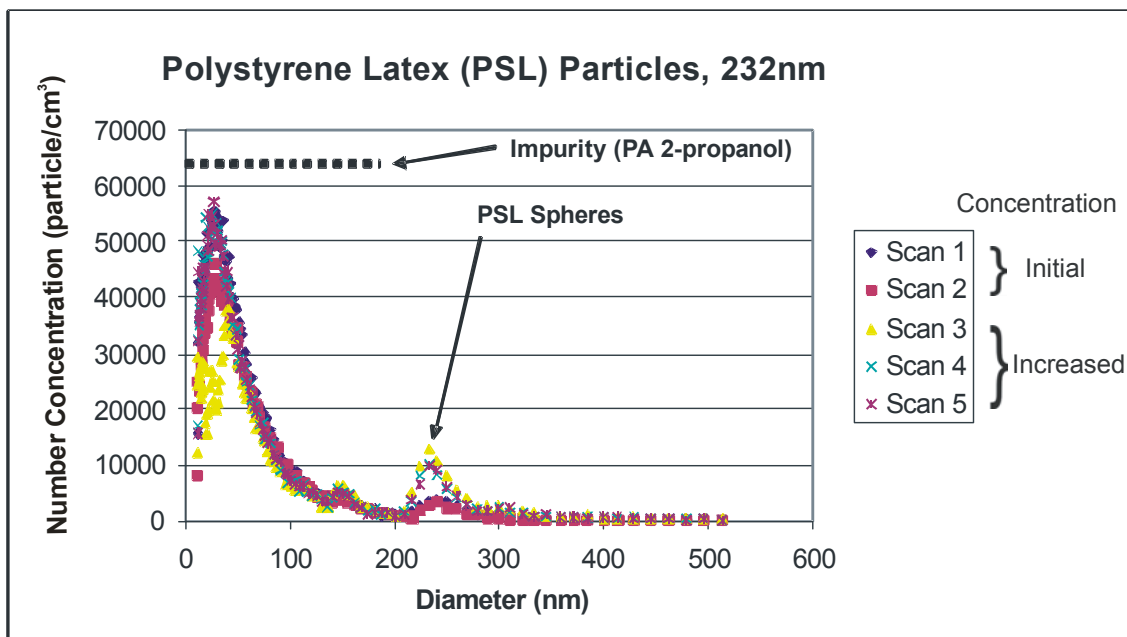


Figure 6: SMPS scans of 232nm PSL spheres dispersed in analytical grade 2-propanol. The concentration of PSL spheres in solution was lower for Scans 1 and 2 in comparison to Scans 3 to 5

All scans exhibit large numbers of particles in the size range below 100nm. The origin of these particles is presumably due to impurities that were present in the solvent, which is supported by ELPI data presented in Section 4.2.3 (Figure 9). It would be possible to reduce this particle count to some extent by multiple distilling of the solvent. The presence of PSL particles is indicated by a peak in the vicinity of 230nm. The concentration of particles in the atomiser was increased after the first two scans, which is reflected by a higher peak in the following scans 3 to 5. Particle numbers below

100nm diameter did not change much, which indicates that these counts were not connected to the addition of PSL.

4.2.2 CNT aerosol characterisation by SMPS

An amount of 0.6 mg of spinnable CNT was originally dispersed in 500ml of 2-propanol to make up the dispersion that was used for this and the following experiments involving synthetic CNT aerosols. The resulting concentration, if fully dispersed, would amount to $4 \cdot 10^7$ fibres/ml in this case.

Figure 7 shows an SMPS data from spinnable CNT when nebulised within the *Test Duct* and sampled from one of the sampling tubes. These data were generated using the manufacturer's propriety software (TSI USA). These current and subsequent SMPS data are presented as number counts per SMPS bin with the particle diameter presented as spherical equivalent electrical mobility diameter. This figure compares the measured particle distribution for the CNT dispersion (CNT + 2-propanol) and for the 2-propanol solvent alone (2-propanol). The scan from an ultra-high purity 2-propanol (Fluka 675431 Chromasolv Plus <0.0001% evaporation residual) is shown as well (UHP Grade 2-propanol) to illustrate the potential for particle background reduction by specialised solvents.

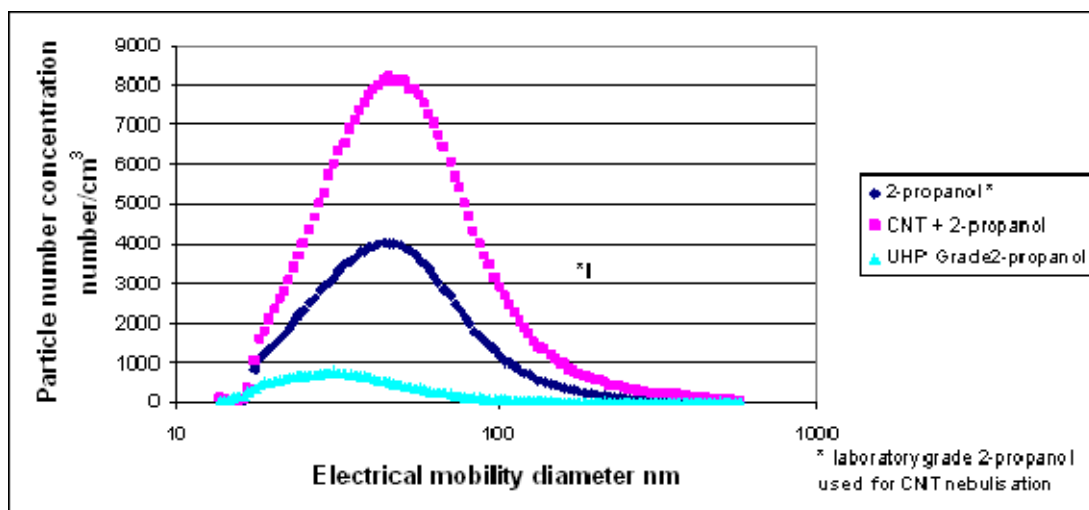


Figure 7: A series of SMPS scans (see Section 3.4.2 for instrument details) from spinnable CNT dispersed in 2-propanol (“CNT + 2-propanol”), the 2-propanol on its own (“2-propanol”) and for an ultra-high purity 2-propanol (“UHP Grade 2-propanol”)

Figure 8 displays the background subtracted particle distribution for spinnable CNT. These SMPS particle distributions of carbon nanotubes are compiled from the average of four 3-minute SMPS scans while the nebuliser was operating at steady conditions (0.04 MPa nozzle pressure) and when the number concentration was relatively constant. The background particle concentration arising from impurities in the 2-propanol solvent has been subtracted as has the background particle concentration from the test rig. This approach relies on the absence of interactions between aerosolised CNT and background particles, which is an approximation.

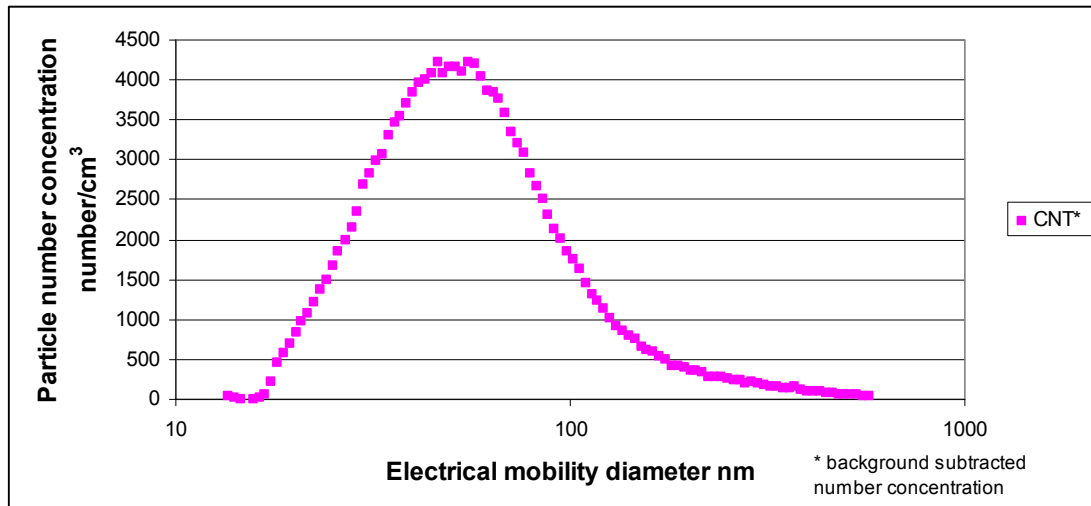


Figure 8: SMPS particle distribution of spinnable carbon nanotubes when nebulised from 2-propanol

4.2.3 ELPI real-time measurements

Spinnable and CCl carbon nanotubes were atomised at 0.04 MPa nozzle pressure and injected into an airstream travelling at 0.6 m·s⁻¹ in the Test Duct. After a travel distance of 1.6 metres, objects formed in the aerosol were sampled by the ELPI to obtain size-resolved data at a time resolution of 1 Hz. SEM and optical microscopy examinations were additionally undertaken on the captured objects for validation of the ELPI electrometer data; these results are discussed in Section 4.2.5.

Figure 9 shows an example of an ELPI measurement while sampling spinnable carbon nanotubes that were nebulised from 2-propanol into the Test Duct (labelled “Spinnable CNT sample”). For comparison and completeness, ELPI measurements for two different 2-propanol samples are also included:

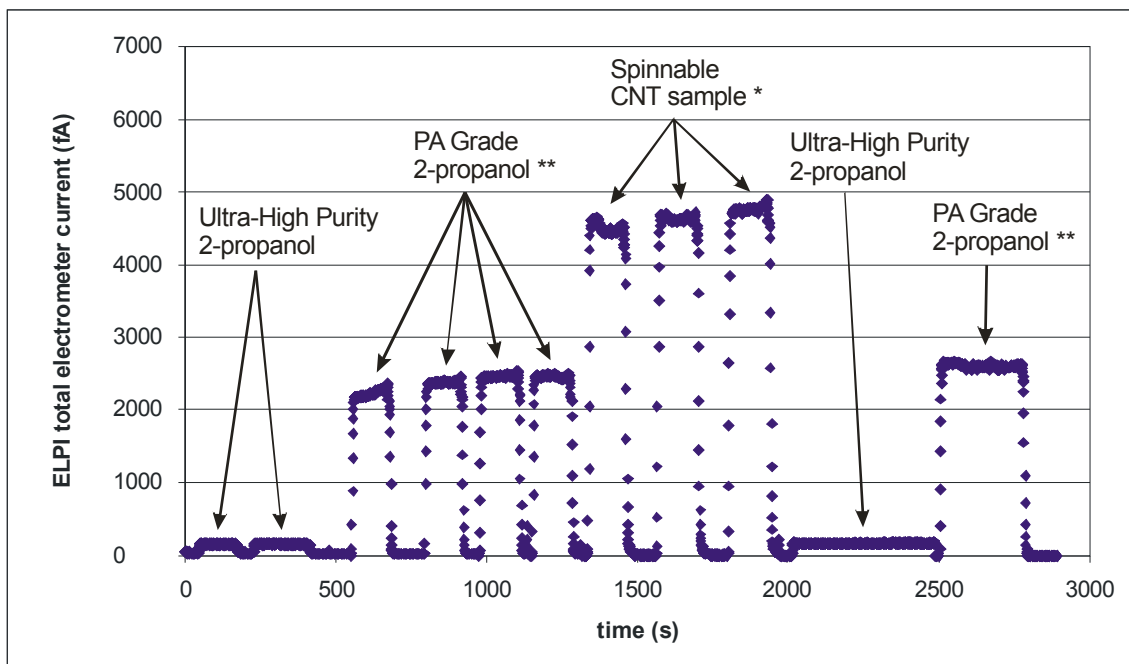
- the analytical grade 2-propanol solvent used to nebulise the carbon nanotubes, as well as
- an ultra-high purity 2-propanol (Fluka 675431 Chromasolv Plus <0.0001% evaporation residual).

The ultra-high purity 2-propanol was used as a baseline solvent for comparing background particle concentrations⁴. To clearly show the background particle concentration within the Test Duct with the nebuliser off as well as the reproducibility of successive particle concentration measurements, the nebuliser was cycled on and off at time intervals of approximately one minute.

These ELPI data present the combined electrometer currents, which can be converted to corresponding total particle number concentrations within the Test Duct (see

⁴ It should be noted that triple-distilled 2-propanol was nebulised between successive measurements to reduce cross contamination between each test sample.

Section 4.2.4). The particle background concentration within the Test Duct when the nebuliser is off can be clearly observed and this is identified as periods where these data approach the zero baseline of this plot. These background particle electrometer currents are of the order of 10-20 fA (10^{-15} Ampères) and relatively small compared to those from the measurements of spinnable CNT. This value is approximately two orders of magnitude less than that of the CNT measurements. The 2-propanol used to nebulise the carbon nanotubes was not a low impurity solvent and so it was expected that the background charge signature of this solvent would be greater than the background charge signature of the ultra-high purity solvent, which was confirmed by the data displayed in Figure 9.



* Spinnable carbon nanotubes suspended and nebulised in 2-propanol.

** Analytical grade 2-propanol solvent used to suspend and nebulise spinnable carbon nanotubes.

Figure 9: ELPI time series of total electrometer current for spinnable carbon nanotubes, the 2-propanol solvent as well as for high purity 2-propanol

The existence of airborne carbon nanotubes within the Test Duct is demonstrated by a clear increase of the electrometer current relative to the low purity solvent “PA Grade 2-propanol”. The observed charge flow from the CNT sample is reproducible and is approximately double that charge current for the 2-isopropanol solvent.

It should be noted that the electrometer current ‘spike’ that is observed at the end and sometimes the beginning of each nebulisation interval occurred as the nebuliser flow was started and stopped and as such it is suspected that this is an artefact of the nebuliser system not operating in steady state. Hence, particle distributions calculated from these data are averaged over the steadier sampling period towards the middle of each of the one minute intervals.

4.2.4 ELPI particle number concentrations

For spherical particles or particles with simple geometries, the calibration function supplied with the instrument can be used to generate particle number concentrations from ELPI currents. Figure 10 displays the background subtracted particle distribution obtained from this calibration function for spinnable CNT that were nebulised within the Test Duct. These ELPI particle distributions of carbon nanotubes are compiled from the average particle distribution while the nebuliser was operating at steady conditions and when the number concentration was relatively constant. The background particle concentration arising from impurities in the 2-propanol solvent has been subtracted as has the background particle concentration from the Test Duct.

As was observed for the SMPS data shown in Figure 8, the ELPI particle number distribution of Figure 10 clearly shows the existence of CNT objects over all ELPI size bins but with small numbers of particles at the larger size ranges.

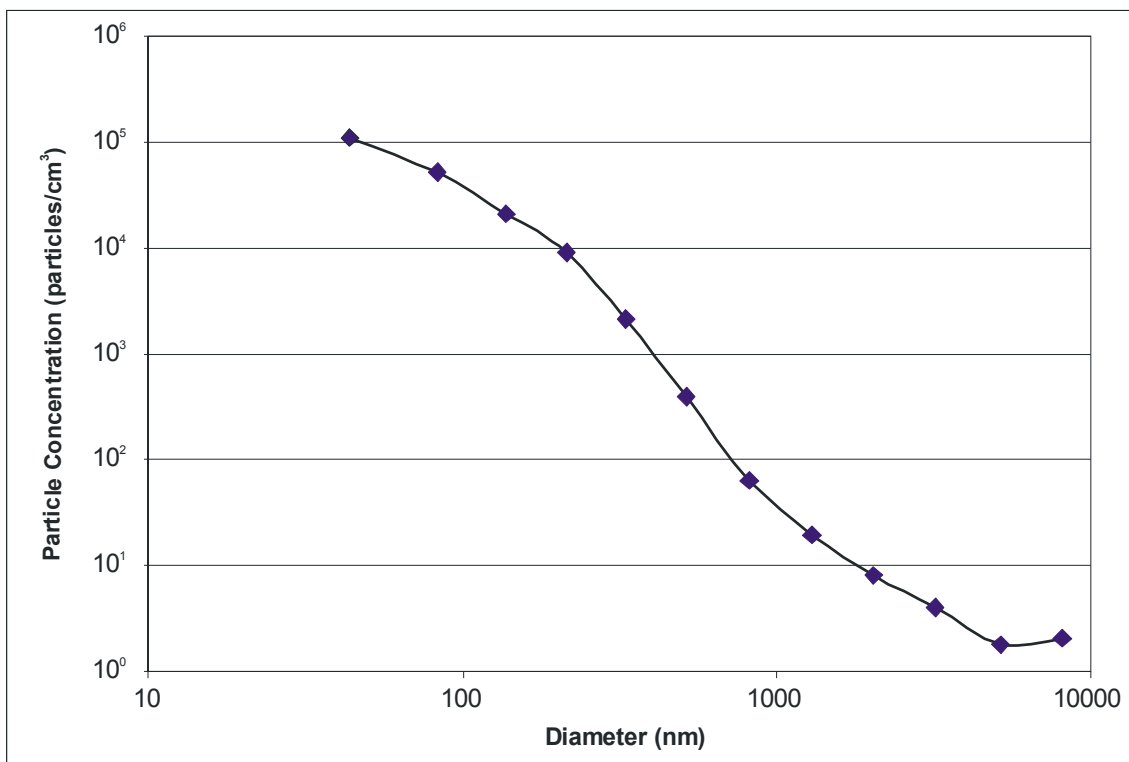


Figure 10: ELPI particle distribution of spinnable CNT when nebulised from 2-propanol

For complex geometries such as CNT a particle dependent calibration is required. It should be noted that this calibration only applies to the real time number concentrations and plays no role in how the particle size fractions are determined during ELPI measurements. The calibration method involves sampling the target particles with the ELPI while simultaneously recording the electrometer currents and then counting the particles deposited on the plate either optically and/or by SEM. This method allows the charge per particle for each ELPI size bin to be deduced and a particle specific ELPI calibration functions to be determined. This process is time

consuming and requires considerable effort to obtain an accurate calibration function. At the time of this report a preliminary ELPI calibration function for CNT had been achieved for some of the coarser particle size bins and using optical microscopy only. These CNT calibration factors have not been thoroughly validated and have therefore not been used or applied to ELPI data in this report. As a result it should be noted that the magnitude of the particle number concentrations displayed in Figure 10 should be considered cautiously until an accurate calibration function is available for CNT objects.

4.2.5 Particle structure information from the ELPI

Spinnable and CCI carbon nanotubes were atomised and injected into an airstream travelling at $0.6 \text{ m}\cdot\text{s}^{-1}$ in the Test Duct. After a travel distance of 1.6 metres, objects formed in the aerosol were sampled by the ELPI. The dust deposits on the plates were subsequently analysed by optical microscopy at CSIRO Lucas Heights and by SEM imaging at CSIRO Belmont and at the Bio21 Institute in Melbourne.

4.2.5.1 Analysis of Spinnable Carbon Nanotubes by Optical Microscopy

Figure 11 shows examples of CNT agglomerates that were deposited on ELPI impactor plate 13. ELPI plate 13 collects objects with a spherical equivalent diameter greater than $10 \mu\text{m}$. The plate was exposed to nebulised spinnable carbon nanotubes for approximately three minutes before examination. This image was obtained with a $6.5\times$ optical magnification and the dimensions of the objects displayed in this image are of the order of millimetres. The image displays five CNT objects and these can be observed as a single object identified within the yellow circle as well as four objects within the black circle.

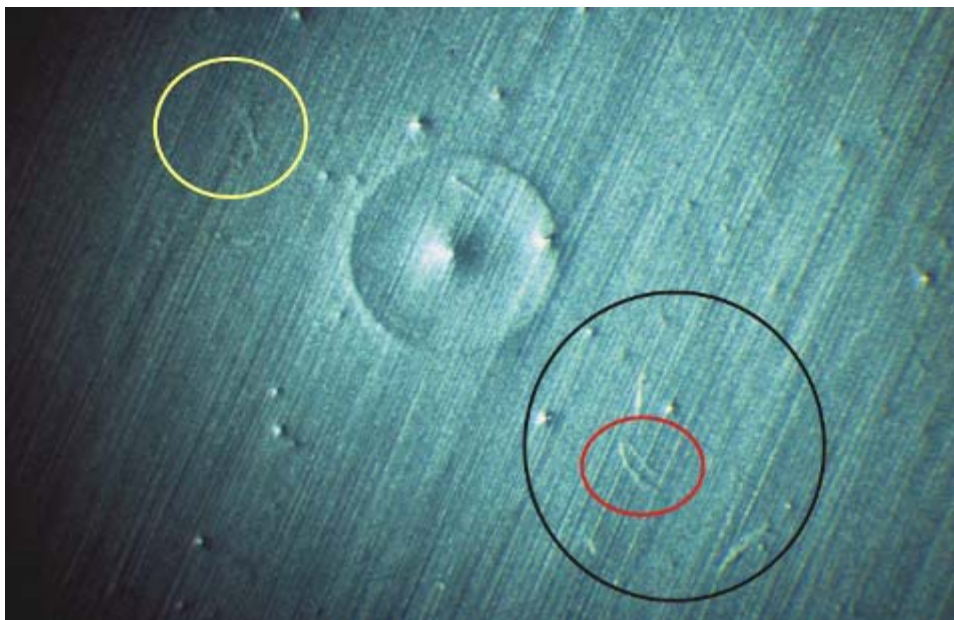
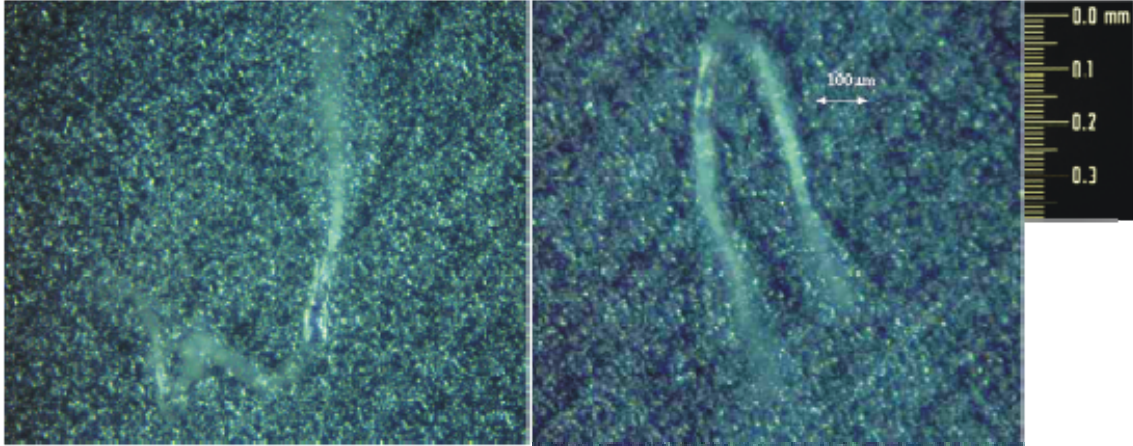


Image by Brendan Halliburton (CSIRO) on Wild M3Z

Figure 11: Optical image of spinnable CNT objects collected on ELPI impactor plate 13. Enlarged views of objects in yellow and red circle are shown in Figure 12

Figure 12 displays the object identified within the yellow circle on the left and that within the red circle on the right at an increased magnification (x400). The CNT objects displayed in both figures exhibit 'yarn like' characteristics and this feature was observed for a number of the objects deposited on ELPI collection plates 5 to 13.



Images by Brendan Halliburton (CSIRO) on wild M3Z (40x instrument magnification with 10x converter in place)

Figure 12: Enlarged optical images of spinnable CNT objects collected on ELPI impactor plate 13 from Figure 11 (400x magnification). The object from the yellow (red) circle is shown on the left (right) side

CNT objects were also observed to be deposited on other ELPI impactor plates. These deposits are normally formed in designated spots on each plate. Figure 13 however shows objects that were deposited at the break in the ends of the circlip ring of ELPI plate 10 that holds the aluminium foil in place, which is rather unusual. ELPI plate 10 collects objects with aerodynamic diameters between 2.5 μm and 4.4 μm.

4.2.5.2 Analysis of spinnable and CCI objects by SEM

Results from SEM imaging of aerosol objects deposited on the impactor plates of the ELPI are shown in Figure 14 and Figure 15. Figure 14 provides images from plates 1 to 4⁵ of structures originating from CCI CNT on the left and compares them to structures generated from spinnable CNT under equivalent conditions, all at the same magnification. This trend is continued in Figure 15 for coarse CCI CNT, comparing pertinent results from plates 4 to 6. Structures formed from fine spinnable CNT, however, are compared in this figure at a higher magnification to make structural changes better visible.

It is interesting to note that TEM images of some CNT bundles reported by NIOSH (Figure 5 in [7]) and by Methner et al. (Figure 2 in [8]) were very similar in shape and structure to the SEM images of the CCI CNT bundles displayed in Figure 15 of this report.

⁵ Plates 1 to 4 collect particles with aerodynamic diameters ranging from 30nm to 260nm (on the basis of D50% values).

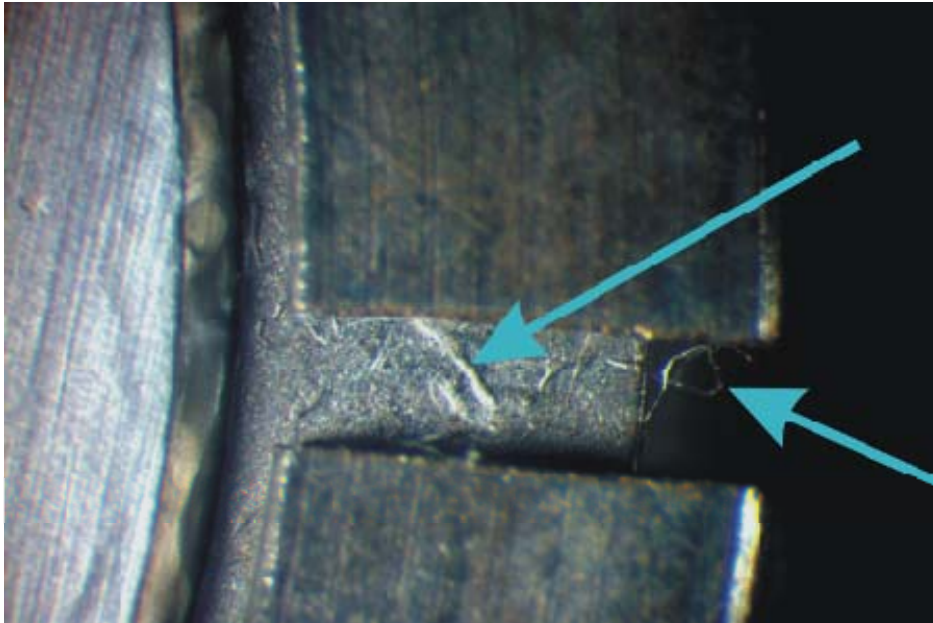


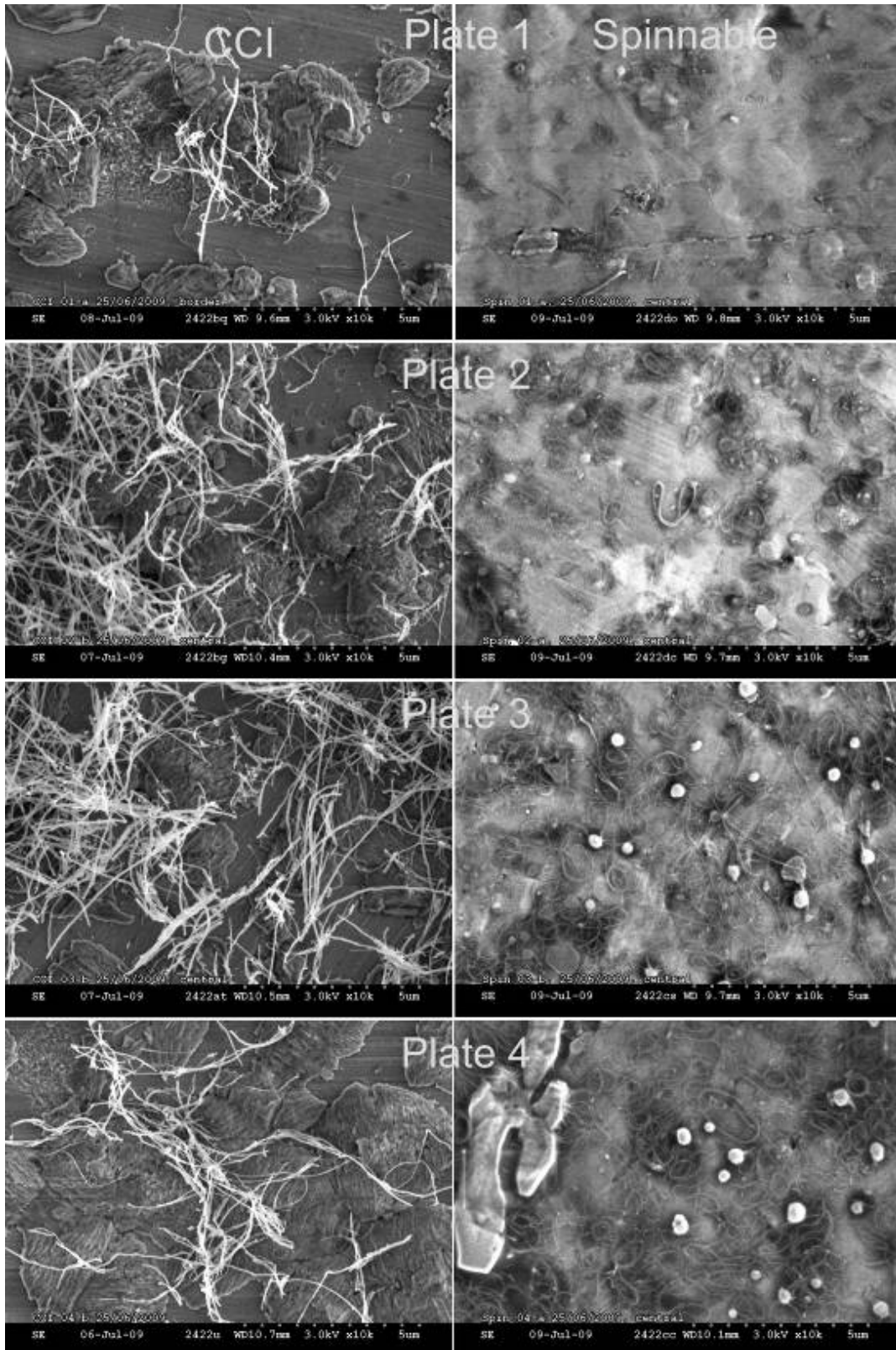
Image by Brendan Halliburton (CSIRO) on Leica DM2500P

Figure 13: Optical image of spinnable CNT objects collected (marked by arrows) on the circlip of ELPI impactor plate 10 (~40x magnification). The aluminium foil substrate can be seen towards the left side of the image

4.2.5.3 About the ELPI collection substrate

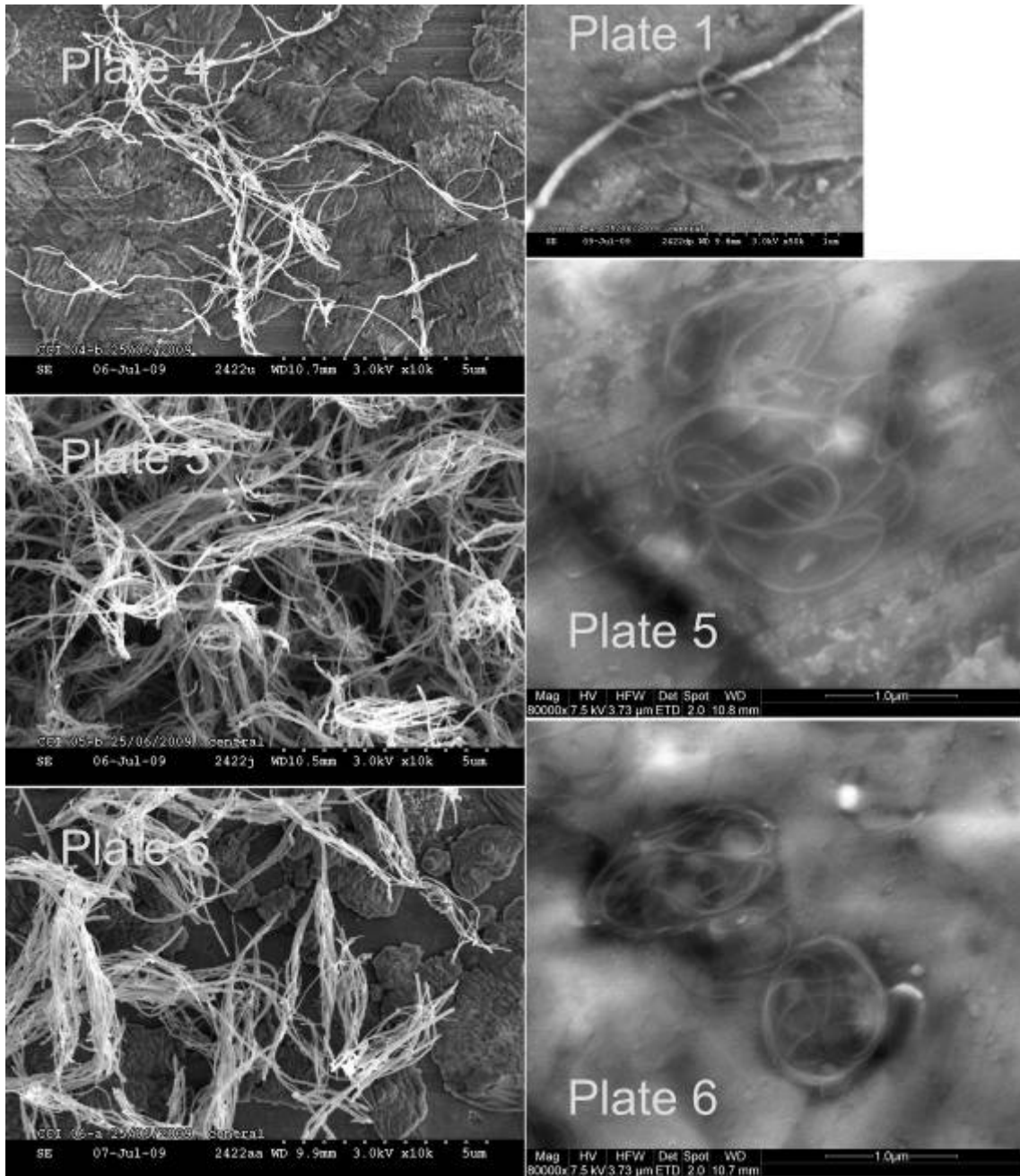
A thin film of grease is commonly applied to the ELPI collection substrate to increase the adhesion of objects during the sampling process and to maintain the integrity of the sample before post sampling analyses are completed. However, while a thin layer of grease was applied to substrates analysed by optical microscopy at the Lucas Heights site, no grease was applied to one set of samples that was designated for analysis by SEM at the CSIRO Belmont site. The plates were used without grease for SEM because the fine CNT objects would otherwise disappear in the thin grease film. The difference in the preparation of impactor plates for optical microscopy (greased) and SEM imaging (not greased) however had a number of consequences:

- It is suspected that the omission of grease for SEM imaging resulted in the larger objects that were initially observed at Lucas Heights site using optical microscopy were not found during SEM imaging. We presume that they got lost during transport to the Belmont site.
- It is known that CNT have a very strong tendency to stick to other CNT or to polymeric surfaces in the immediate neighbourhood. However, since the ELPI substrate consists of an aluminium foil, this observation suggests that the larger dimensioned CNT may be relatively easily lost from the metallic surface of metal collection substrates.



SEMs by Colin Veitch (CSIRO) on Hitachi S4300SE/N

Figure 14: SEM images of CCI CNT (left) and Spinnable CNT (right) collected on ELPI impactor plates 1 to 4 (all at the same magnification)



Left: SEMs by Colin Veitch (CSIRO) on Hitachi S4300SE/N . Right: SEMs by Roger Curtain (Bio21) and Jurg Schutz (CSIRO) imaged on FEI Quanta 200F at the Bio21 Institute

Figure 15: SEM images of CCI CNT of large size (left) and an illustration of the size range observed for Spinnable CNT at high magnification (right)

4.2.5.4 Summary of CNT objects observed

- Optical microscopy undertaken at CSIRO Lucas Heights in Sydney revealed the existence of objects resembling ‘yarn-like’ agglomerates (Figure 11 to Figure 13 in Section 4.2.5.1). These objects were observed to have physical dimensions ranging from microns to millimetres but with spherical equivalent aerodynamic

diameters ranging from approximately 500nm to greater than 10,000nm. Each image had been obtained from one and the same CNT experiment.

- While these larger dimensioned CNT objects were observed to have deposited on most of the ELPI collection plates, these objects tended to be deposited in fewer numbers on the ELPI plates with object size cuts of less than approximately 0.5 μ m.
- SEM imaging undertaken at CSIRO Belmont in Geelong of CNT aerosol objects deposited on the ELPI plates (Figure 14 and Figure 15 in Section 4.2.5.2) revealed the existence of deposits on the lowest six size plates of the ELPI only, which have maxima of modal diameters distributions of 43.5nm for plate 1, 83nm for plate 2, 137nm for plate 3, 215nm for plate 4, 330nm for plate 5 and 516nm for plate 6.

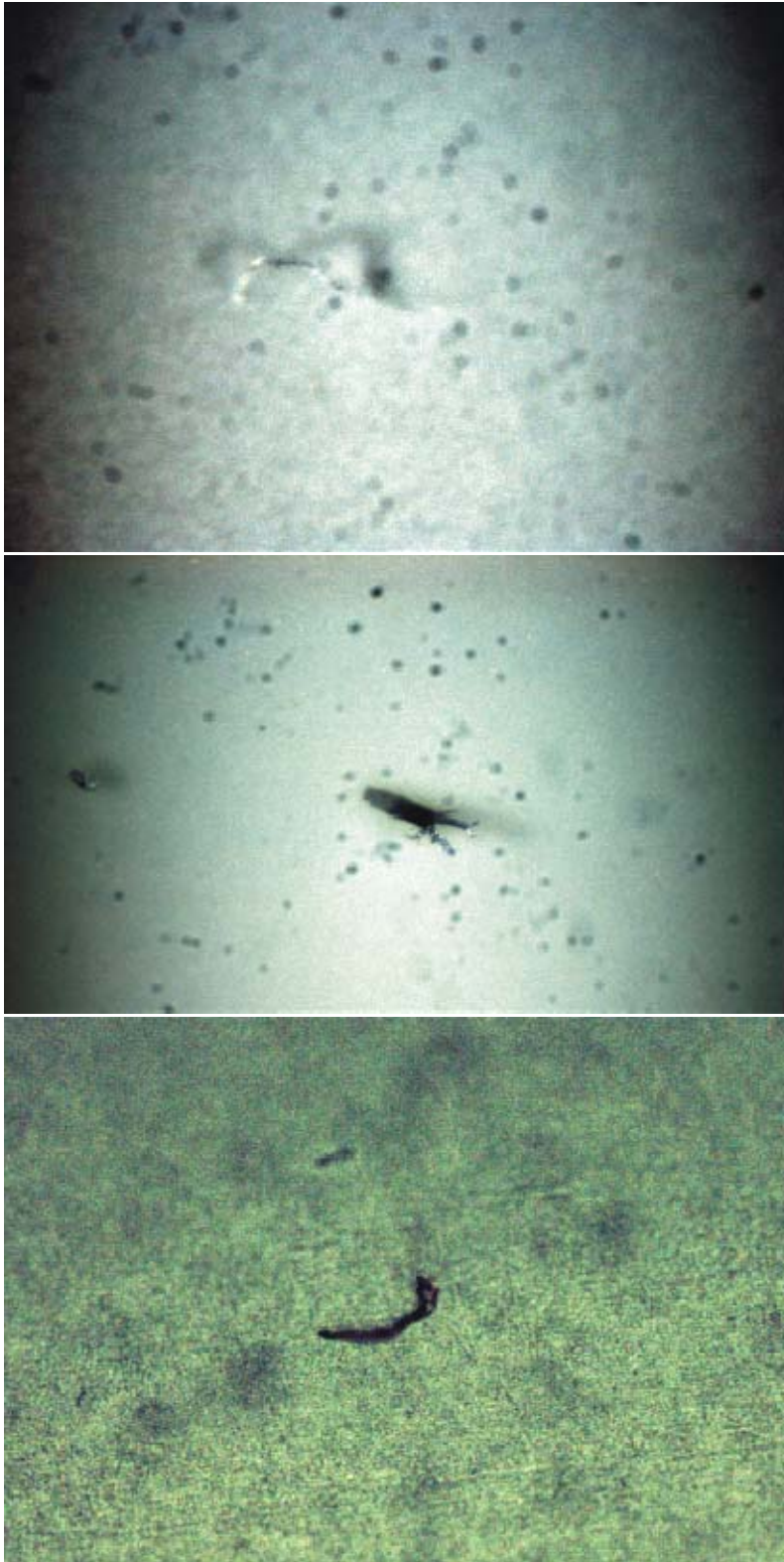
4.2.6 Membrane-based sampling of synthetic CNT objects

The presence of CNT aerosol objects in the airstream of the Test Duct was verified by means of membrane-based sampling.

The first experiment followed conventional particle sampling techniques that are prescribed for the extractive sampling of particles within industrial systems [33] to extract spinnable CNT objects via one of the 3/8" sampling tubes of the Test Duct. The objects were captured on an uncoated polycarbonate filter membrane of 47mm diameter and 0.22 μ m pore size. The membrane was maintained in a horizontal orientation with the objects being drawn downward onto the filter medium.

Optical microscopy revealed the presence of larger CNT constructs on the membrane surface, but does not have the capacity to detect small CNT objects. Figure 16 displays three separate examples of CNT objects deposited onto this polycarbonate membrane during the simple filter experiment. Figure 17 displays a series of three images taken at greater resolution from one and the same CNT object, but from three different focal planes.

In the second experiment, the objects from spinnable CNT were sampled from the Cowl Chamber of the Test Duct at a reduced face velocity. The stainless steel cowl of the Test Duct (see Figure 3 and sketch of Figure 19) was used to sample CNT aerosol objects onto a gold coated polycarbonate membrane with 100nm pore diameter at a flow rate of 1 LPM. The stainless steel cowl had a diameter of 25mm and was oriented normally with the opening pointing downwards to reproduce the set up used during the sampling in the CNT Yarn Spinning Laboratory. The orientation of the sampling cowl was also changed to point upwards in order to establish the influence of gravity on particle capture. The duration of the sampling was ten minutes with cowl pointing downwards and two minutes with the cowl pointing upwards. Optical images of respective membrane surfaces are shown in Figure 18, showing on the left side results from the cowl pointing downwards and on the right side those from the cowl pointing upwards. The number of objects found on the membranes was clearly higher when the cowl was pointing upwards, which suggests that the orientation of the cowl introduces some form of size selectivity for the larger agglomerates.



Images by Brendan Halliburton (CSIRO) on Leica DM2500P

Figure 16: Optical images of CNT objects deposited on the polycarbonate membrane from an airstream sampled through a 3/8" sampling tube (10x magnification)



Image by Brendan Halliburton (CSIRO) on Leica DM2500P

Figure 17: A series of optical images taken to highlight the detailed structure of the CNT object

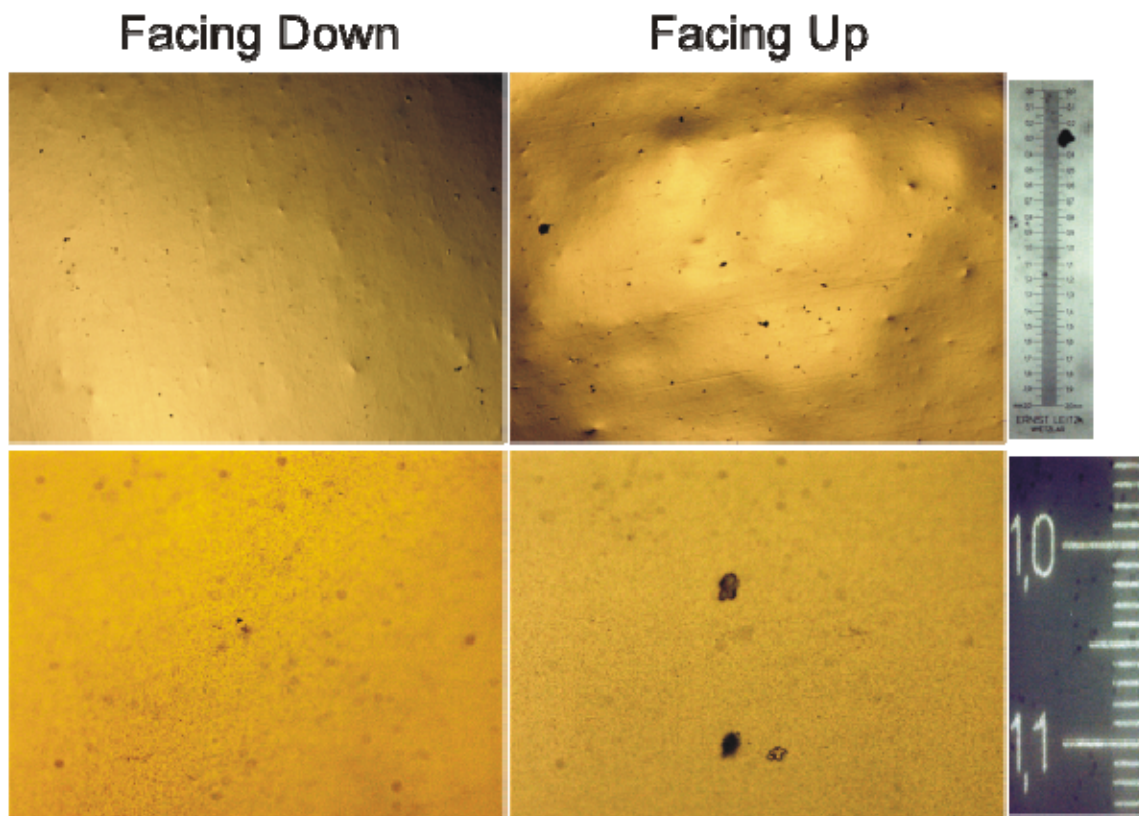


Image by Brendan Halliburton (CSIRO) on Leica DM2500P

Figure 18 Optical microscope images of CNT objects found on gold-coated membrane surfaces from sampling of CNT aerosols by the cowl of the Test Duct. Images on the left (right) show membrane surfaces where the cowl had been pointing downwards (upwards). Scale bars in millimetres are provided on the right border: the magnification in the upper row was 4x and 50x in the bottom row

5 Discussion

5.1 Information from real-time data

5.1.1 CNT yarn spinning laboratory

An analysis of data sampled in February 2009 found no unusual levels of particles in the background (Section 4.1.2) other than particles from the vacuum pump of the ELPI. It was possible to reduce levels of these particles by venting the exhaust from the vacuum pump through a fume cabinet. There were also no changes in measured particle size distributions, which could be attributed to the operation of the CNT Yarn Spinner.

5.1.2 SMPS measurements in test duct

Figure 8 shows the measured SMPS particle size number distribution obtained from a nebulised dispersion of spinnable CNT in 2-propanol inside the Test Duct. These results clearly indicate the existence of CNT particles in the airstream with a main size range span of approximately 16nm to 150nm and a peak in the vicinity of 50nm. The distribution has a distinct tail on the coarse end of the particle size number distribution that reaches up to 500nm.

Tsai et al. measured the particle number distribution at the exhaust of their single-wall CNT reactor (Figure 2 in [12]) by means of a Fast Mobility Particle Sizer (FMPS), an instrument that follows similar principles to the SMPS. Their measured distribution for single-walled CNT is similar to ours for fine MWCNT, with a peak in the vicinity of 50nm, and very similar particle size end points. The main difference is that Tsai et al. did not observe the tail from 100nm to 500nm at the coarse end of the distribution shown in our Figure 8.

5.1.3 ELPI measurements in test duct

The approximate size dependence of CNT objects in the aerosol is shown in the ELPI particle number distribution of Figure 10. The distribution clearly shows the existence of CNT objects over all ELPI size bins but with small numbers of particles at the larger size ranges. It should be noted that the magnitude of the particle number concentrations displayed in Figure 10 should be considered cautiously until an accurate calibration function is available for CNT objects.

5.2 Structure information for CNT objects from the ELPI

Overall, these measurements clearly reveal the existence of large numbers of CNT in sampled synthetic aerosols from the Test Duct. However, it is currently unclear whether the larger dimensioned deposits that were found by optical microscopy on the smaller object diameter sizing plates arise from particle bounce⁶ or are a true measure of the spherical equivalent diameter of the objects. Clearly this aspect requires further investigation if the penetration function into the lung is to be accurately understood.

Detailed high magnification images of the larger CNT objects were difficult to achieve by optical microscopy as the entire structure of the object could not be resolved within the focal plane of the microscope. Hence the sections of the object located above and below the focal plane appear blurred.

It is suspected that the omission of grease for SEM imaging resulted in the larger objects that were initially observed at Lucas Heights site using optical microscopy were not found during SEM imaging. It is known that CNT have a very strong tendency to stick to other CNT or to polymeric surfaces in the immediate neighbourhood. However, since the ELPI substrate consists of an aluminium foil, this observation suggests that the larger dimensioned CNT are relatively easily lost from the metallic surface of metal collection substrates.

CCI CNT are generally easy to spot on SEM images. On the basis of images from Figure 14 there is no clear change in agglomeration state visible between impactor plates 1 to 4. Results from plates 5 and 6 in Figure 15 however show clear agglomerates in the form of bundles. These bundles are typically 1µm in diameter and approximately 5µm long.

The structure of objects generated from spinnable CNT, on the other hand, almost always has the shape of a coil. The coils found on plate 1 are approximately 0.5µm by 1µm in size. The dimensions of coils found on plates 2 to 6 do not change much in comparison to those from plate 1. It seems though that their aerodynamic diameter is larger because the coils have a larger number of “windings”. This may be because the CNT are longer or the result of a larger number of individual CNT in the coil. It is also difficult to predict the ‘in-flight’ geometry following impaction onto the aluminium foil as one is trying to interpolate a three dimensional shape from an essentially two dimensional image.

It is therefore possible to conclude that aerosol objects generated from CCI CNT clearly differ from those of spinnable CNT. While coarse CCI CNT either travel as individual fibres or bundles of fibres, fine spinnable CNT form coils that vary in aerodynamic diameter, but are fairly uniform in size. It should also be noted that these structures may be substantially different for aerosols generated by processes other than atomisation.

⁶ Particle bounce describes a process where particles in an airstream are hitting the target plate of an impactor stage and bounce back into the airstream, rather than stick to the impactor plate.

5.3 Membrane-based sampling

5.3.1 Analysis of air samples from CNT yarn spinning laboratory

Extensive inspection of the two gold-coated polycarbonate membranes used during air sampling on 26 February 2009 has so far not produced any evidence of spinnable CNT. The SEM frame shown in Figure 5 illustrates the typical nature of the membrane surface, which had been exposed to sampled air from above the yarn spinning head for 87 minutes. Only fibres of much larger size, cell-like structures and particles were found.

This result therefore requires a detection limit to be established on the basis of a zero count for the objects of interest. Details of this process are provided in Appendix E. To calculate the detection limit (DL) we multiply the sensitivity S with $\mu_0 = 3.00$ (for 95% confidence). We report the structure count in the CNT Yarn Spinning Laboratory on 26 February 2009 as “below detection” with a detection limit of 19.9 fibres/cm³.

The general scenario for spinnable CNT of 10nm diameter indicates that it is possible to reach a Detection Limit of 1 fibre/ml (for a power of 95%) by means of significant but reasonable effort. The effort involved would include:

- 6 hours of sampling at 2 LPM ($V = 720 \cdot 10^3 \text{ cm}^3$), and
- an investigation of 100 SEM fields.

This takes approximately six to nine days of work, including one day for air sampling, one to two days for taking SEM images and four to six days for analysing them.

The means available to reduce the Detection Limit to lower values therefore appears to be quite limited: one may consider counting more fields or conduct sampling over several days. The flow rate can also be raised if it is possible to increase the pore size of the polycarbonate membrane without losing fibres.

It is interesting to note in this regard that other authors reported having detected significantly lower fibre concentrations than the 1 fibre/ml proposed here (see e.g. Table 2 in [9]). Han et al. applied NIOSH TEM method 7402 [24] to the analysis of their samples, which uses mixed cellulose ester membranes without plasma ashing (Table 1). It should be noted that the MWCNT detected in those work environments were significantly coarser (55nm in [9] compared to 10nm in this report) and it was possible to work with a magnification of ca. 10,000, compared to 60,000 required for spinnable CNT. Another factor is the smaller membrane pore size of 100nm for this work, in comparison to the 800nm pore size used by Han et al., which imposes a greater restriction on fluid flow.

5.3.2 Analysis of synthetic CNT objects

From experiments conducted with the ELPI in the controlled environment provided by the Test Duct, where particles other than the synthetically generated CNT aerosol

objects are largely excluded, it has been possible to show that such aerosols can be generated from spinnable CNT as well as from CCI CNT by means of atomisation (sections 4.2.3 and 4.2.5). Total number counts from particle distributions measured by SMPS (Figure 8) and ELPI (Figure 10) indicate that concentrations of around $5 \cdot 10^5$ structures per cm^3 are generated in the Test Duct at an atomiser nozzle pressure of 0.04 MPa. An uncoated polycarbonate membrane was connected to the sampling port of the ELPI to verify that the selected membranes are applicable to capturing synthetic CNT aerosols. The deposits on the membrane surface were analysed by optical microscopy only (Figure 16 and Figure 17).

The stainless steel cowl from the Cowl Chamber of the Test Duct (see Figure 3 and sketch of Figure 19) was used during the experiment reported in Section 4.2.5.2 to sample CNT aerosol objects onto a gold coated polycarbonate membrane with 100nm pore diameter. This was the same type of membrane that was used for sampling in the CNT Yarn Spinning Laboratory, as discussed in Sections 3 and 4 of this report. This led us to conclude that no spinnable CNT had been identified that were due to a release of such objects by the yarn spinning process.

It was the purpose of a second series of experiments that used the stainless steel cowl inside the Cowl Chamber of the Test Duct to evaluate the sensitivity of the membrane technique to the different types of CNT aerosols.

The selected sampling rate for the Test Duct cowl was 1 LPM; in comparison, the flow rate used for membrane-based sampling in the Yarn Spinning Laboratory was 2 LPM. The duration of the sampling varied between 15 seconds and 10 minutes, which was comparable to sampling time used for the ELPI when it sampled those very same synthetic CNT aerosols, but significantly shorter than the 87 minutes of sampling from the experiment in the Yarn Spinning Laboratory. The shorter sampling time was however more than offset by a larger structure density of $5 \cdot 10^5$ structures per cm^3 in the Test Duct.

The gold coated membranes from the cowls were analysed by optical microscopy not far away from where the Test Duct was located to reveal the presence and structure of coarse CNT objects. Some of these results are shown in Figure 18. Results clearly show the presence of large CNT objects on the membrane surface for the cowl oriented pointing upwards as well as downwards. The concentration of particles does however seem to be higher when the cowl is oriented pointing upwards.

5.4. Implications of findings for detecting carbon nanotubes

The synthetic CNT aerosol characterisation work was undertaken in the Test Duct at very high concentrations of CNTs in Nitrogen ($5 \cdot 10^5$ structures per cm^3), with limited background contamination and variation in background particle levels. The full range of CNT size fractions were detected by SMPS, ELPI and ELPI particle collection on plates, while filter membranes in a stainless steel cowl set up were shown to collect larger CNT objects.

However, further work is needed to determine whether these methods would be successful at detecting CNTs in workplace settings at low concentrations and with varying levels of non-fibrous background particles. Different methods may be needed to optimally collect and detect fine CNT (SWCNT, and fine MWCNT) and coarser MWCNT as their differing properties such as flexibility, stickiness, electrostatics and other physical properties may affect collection and detection efficiencies.

Experimental considerations are:

A. For membrane sampling

- Membrane type – collecting particles on the membrane surface minimises the effect of disturbances from subsequent preparatory treatments but may be subject to increased particle loss during general handling.
- Cowl orientation – cowl pointing upwards appears to collect more particles.
- Membrane coating – some evidence that CNT may be lost from metallic surfaces.
- Pore size – larger pore size will allow larger sampling volume.

B. For SMPS and ELPI

- Calibration – instruments require CNT-specific calibrations.
- Atomisation – requires use of ultra-pure dispersion solvents to minimise ultrafine particle background.

This range of instruments typically cost well in excess of AUD \$100,000 and specific training is needed for their operation.

The Electrostatic Low Pressure Impactor (ELPI) has the capacity to capture aerosol particles from large volumes of air and form a concentrated deposit of captured particles over a small area. This ability is very valuable because it addresses the shortcomings of membranes, where limitations on sampling rate (via the pore size required to capture nanoparticles) and sampling time (via eight hour working days) determine the volume of sampled air that can be processed. It also allows imaging of particles after collection to determine if fibrous structures of concern are present.

6 Summary

Aerosol monitoring investigations have been conducted in the Carbon Nanotube (CNT) Yarn Spinning Laboratory at CSIRO in Belmont with the objective to determine typical object concentrations for airborne CNT from the spinning process.

None of the experiments has so far produced evidence of airborne spinnable CNT. It was, however, possible to determine a detection limit from membrane sampling experiments that acts as an upper limit for airborne CNT fibre objects. This detection limit for very fine spinnable CNT is currently at 20 fibres/ml for the sampling parameters used in this investigation and for the number of SEM frames processed (Section 5.3.1, Appendix E), but it would be possible to lower this limit to 1 fibre/ml with reasonable effort. Current experience suggests that further lowering of the detection limit below 1 fibre/ml would be very time consuming if this particular method was used in its current form. This limit is significantly higher than that reported by other authors which most probably is due to:

1. the smaller diameter of the MWCNT used in this experiment, and,
2. the smaller pore size of the membranes used in the sampling cassettes.

Regarding microscopy of fine, spinnable CNT on gold coated polycarbonate membranes the following points are noted:

- Spinnable CNT should be imaged at magnification 60,000 to ensure that individual CNT or thin CNT bundles are not missed.
- Spinnable CNT are relatively easy to distinguish from particle background because they clearly differ in shape and size from typical background objects. CCI CNT, on the other hand, are hard to distinguish from mineral fibres that occur quite regularly in natural particle background.
- Counting experiments conducted on SEM images of gold coated polycarbonate membranes with known amounts of spinnable CNT fibres deposited suggest that each CNT had been broken on average into 50 pieces. The likely cause for the rupturing was the ultrasonic treatment that was used for dispersing the CNT in 2-propanol.

A particle-proof containment was built to allow a more detailed study of CNT aerosols in a safe environment that remains undisturbed from particle background. To test the containment, aerosols of polystyrene latex (PSL) were generated using an atomiser and released into a gas stream of nitrogen from where they were sampled by means of sampling tubes. CNT aerosols were generated from dispersions of spinnable CNT and coarser CCI CNT in 2-propanol. Results from ELPI and SMPS measurements show that such objects are successfully atomised inside the Test Duct and registered by the air sampling equipment.

Carbon nanotubes have been successfully nebulised within the low background testing environment and measurable object concentrations of spinnable CNT objects have been produced. The particle concentration in the test set up was approximately $5 \cdot 10^5$

structures per cm^3 as determined from total number counts measured by the SMPS and the ELPI. It has been shown that the spinnable CNT sample contained a wide range of object sizes with spherical equivalent aerodynamic diameters from 10nm to more than 10 μm . The existence of the nebulised CNT has been validated by both optical microscopy and by SEM.

7 Relation of this CNT Detection Work to Other Work and Approaches

The OECD Working Party on Manufactured Nanomaterials (WPMN) has developed guidance on the initial assessment of emissions from nanomaterial processing [17]. This is based on the use of three techniques: CPC, OPC and membrane sampling – with other sampling being optional on top. This approach (using a TSI 3007 CPC, an ART Instruments HHPC-6 OPC and sampling according to NIOSH Method 7402) has been used successfully by Johnson et al. [34] to detect and evaluate emissions from water suspensions of various carbon-based nanomaterials (including fine CNT of 10-20nm diameter) from laboratory processes.

Similar techniques were used as part of initial investigations in CSIRO's Belmont Laboratories to investigate emissions from the CNT yarn spinning process, but no CNT were detected (Section 4.1). This led researchers to question:

1. Are there no CNT emitted as aerosols? or
2. Are there problems with the methodology used in detecting emissions of the very fine, spinnable CNT?

Thus a more detailed investigation was undertaken that involved the use of a Scanning Mobility Particle Sizer (SMPS) and an Electrostatic Low-Pressure Impactor (ELPI) – but again, no CNT were detected (Sections 4.1.1 and 4.1.2). The uncertainty in relation to questions 1 and 2 above had not been resolved.

To check the sensing potential of the methodology, a Hazardous Aerosol Test Duct was built that allowed safe handling of hazardous aerosols (Appendix A). Results from the use of ELPI and SMPS to examine CNT aerosols showed clearly that airborne fine, spinnable CNT can be detected by these instruments in real-time and that CNT structures from only a few CNT to larger constructs are collected on the ELPI impactor plates (Section 4.2).

Thus, there may be potential to use an ELPI for further investigations in workplace settings. Possibly, it could be used for confirmation where no material is detected using the OECD WPMN initial assessment guidance. It has the advantage of being able to capture aerosol particles from large volumes of air and form a concentrated deposit over a small area.

8 Conclusions and Issues for Further Consideration

Reports on workplace assessments that cover the use of carbon nanotubes (CNT) are available in the literature from a number of authors ([6],[7],[8],[9],[10],[11],[12]).

Sampling cassettes constitute one method that is generally used in such investigations. The pore size of the membranes used in the cassettes needs to be appropriate to collect those particles that are to be investigated. Finer pores do however impose a more stringent limit on the amount of air that can be drawn through the membrane. Investigations reported here suggest that a membrane pore size of 100nm may be limiting the sensitivity that can be reached with reasonable effort to a level where it is not possible to determine if a workplace is safe.

One of the main obstacles that limit the capacity to detect low levels of CNT in ambient air for real time sampling equipment is the naturally occurring nanoparticle background, which also tends to vary significantly over time. An approach that has been widely adopted to mitigate this problem is to compare real time measurements from an active source of CNT aerosols to the normally occurring particle background. There are different ways to conduct such comparisons, which are discussed in detail in reference [18], but the limiting impact of the issue on the sensitivity of the technique remains considerable.

Impactor-based systems such as an Electrostatic Low Pressure Impactor (ELPI), a Micro-Orifice Uniform Deposit Impactor (MOUDI) or a Nanosampler have the capacity to capture aerosol particles from large volumes of air and form a concentrated deposit of captured particles over a small area. This ability is very valuable because it addresses the shortcomings of membranes, where limitations on sampling rate (via the pore size required to capture nanoparticles) and sampling time (via eight hour working days) determine the volume of sampled air that can be processed. It also allows imaging of particles after collection to determine if fibrous structures of concern are present, which addresses the lack of structural information from systems like Scanning Mobility Particle Sizers (SMPS).

But even with sound methods for assessing particle size, such as can be provided by many of the real time and impactor based systems, it is currently not possible to obtain information on particle structure and particle concentration at the same time. However, this information is necessary if one needs to assess exposure in the workplace to specific particles, such as fibrous objects or other particles that are more hazardous than typical background particles.

A number of issues have emerged from this work that require further investigation or consideration:

1. Most important is to understand the factors that impact on the detection limit for membrane filter sampling, and to reduce the detection limit below levels determined in this study.

2. It may be useful to use “monodisperse” CNT aerosols⁷ and investigate in more detail the fibre-specific signatures that the detecting instruments may have [35]. Comparisons between these signatures may give some indication of the fibre content in a background of otherwise essentially spherical objects.
3. Background-free test aerosols can also be useful for assessing in detail the sensitivity of membrane-based sampling for aerosols of nanoparticles other than carbon nanotubes. This includes measurements that specify the minimum requirement for membrane pore size that ensures particles are not lost.
4. There have been novel developments in filter media with specific designs for fine and nanoparticle capture. Parameters such as microfibrils, nanofibrils, and electrostatic charge could be investigated individually and in combination on aerosols in the background-free Test Duct.

⁷ “Monodisperse” equivalents for CNT could be generated for example from CNT forests grown to well-defined lengths from CNT with well-defined diameters by dispersing them in a compatible solvent at short exposure to ultrasound. The effect of fibre fracture needs to be determined.

References

- [1] Poland CA., Duffin R, Kinloch I, Maynard A, Wallace WAH, Seaton A, Stone V, Brown S, MacNee W, and Donaldson K. "Carbon Nanotubes Introduced into the Abdominal Cavity of Mice Show Asbestos-Like Pathogenicity in a Pilot Study." *Nature Nanotechnology* 3, no. 7 (2008): 423-28.
- [2] Ryman-Rasmussen JP, Cesta MF, Brody AR, Shipley-Phillips JK, Everitt JI, Tewksbury EW, Moss OR, Wong BA, Dodd DE, Andersen ME, and Bonner JC. "Inhaled Carbon Nanotubes Reach the Subpleural Tissue in Mice." *Nature Nanotechnology* advance online publication (2009).
- [3] Porter AE, Gass M, Muller K, Skepper JN, Midgley PA, and Welland M. "Direct Imaging of Single-Walled Carbon Nanotubes in Cells." *Nature Nanotechnology* 2, no. 11 (2007): 713-17.
- [4] International Organization for Standardization. *Ambient Air - Determination of Numerical Concentration of Inorganic Fibrous Particles - Scanning Electron Microscopy Method*. ISO 14966:2002(E). ISO, (2002).
- [5] Yang W, Peters JI, and Williams RO. "Inhaled Nanoparticles - A Current Review." *International Journal of Pharmaceutics* 356, no. 1-2 (2008): 239-47.
- [6] Maynard AD, Baron PA, Foley M, Shvedova AA, Kisin ER, and Castranova V. "Exposure to Carbon Nanotube Material: Aerosol Release During the Handling of Unrefined Single-Walled Carbon Nanotube Material." *Journal of Toxicology and Environmental Health-Part a* 67, no. 1 (2004): 87-107.
- [7] National Institute for Occupational Safety and Health. *NIOSH Health Hazard Evaluation Report: HETA No. 2005-0291-3025, University of Dayton Research Institute, Dayton, Ohio, October 2006*. PB2007103039. (2007). <http://hdl.handle.net/123456789/6932>.
- [8] Mazzuckelli LF, Methner MM, Birch ME, Evans DE, Ku BK, Crouch K, and Hoover MD. "Identification and Characterization of Potential Sources of Worker Exposure to Carbon Nanofibers During Polymer Composite Laboratory Operations." *Journal of Occupational and Environmental Hygiene* 4, no. 12 (2007): D125-D130.
- [9] Han JH, Lee EJ, Lee JH, So KP, Lee YH, Bae GN, Lee S-B, Ji JH, Cho MH, and Yu IJ. "Monitoring Multiwalled Carbon Nanotube Exposure in Carbon Nanotube Research Facility." *Inhalation Toxicology* 20, no. 8 (2008): 741-49.
- [10] Bello D, Hart AJ, Ahn K, Hallock M, Yamamoto N, Garcia EJ, Ellenbecker MJ, and Wardle BL. "Particle Exposure Levels During Cvd Growth and Subsequent Handling of Vertically-Aligned Carbon Nanotube Films." *Carbon* 46, no. 6 (2008): 974-77.
- [11] Bello D, Wardle BL, Yamamoto N, Devilloria RG, Garcia EJ, Hart AJ, Ahn K, Ellenbecker MJ, and Hallock M. "Exposure to Nanoscale Particles and Fibers During Machining of Hybrid Advanced Composites Containing

Carbon Nanotubes." *Journal of Nanoparticle Research* 11, no. 1 (2009): 231-49.

- [12] Tsai SJ, Hofmann M, Hallock M, Ada E, Kong J, and Ellenbecker M. "Characterization and Evaluation of Nanoparticle Release During the Synthesis of Single-Walled and Multiwalled Carbon Nanotubes by Chemical Vapor Deposition." *Environmental Science & Technology* 43, no. 15 (2009): 6017-23.
- [13] ASTM International. *Standard Practice for Sampling and Counting Airborne Fibers, Including Asbestos Fibres, in the Workplace, by Phase Contrast Microscopy (With and Option of Transmission Electron Microscopy)*, D 7201 - 06. IHS, (2006).
- [14] National Occupational Health and Safety Commission. *Guidance Note on the Membrane Filter Method for Estimating Airborne Asbestos Fibres*, [NOHSC:3003(2005)]. Commonwealth of Australia, Canberra, ACT Australia, 2005.
- [15] International Organization for Standardization. *Ambient Air - Determination of Asbestos Fibres - Direct-Transfer Transmission Electron Microscopy Method*. ISO 10312:1995(E). ISO, (1995).
- [16] ASTM International. *Standard Test Method for Airborne Asbestos Concentration in Ambient and Indoor Atmospheres As Determined by Transmission Electron Direct Transfer (TEM)*, D 6281 - 06. IHS, (2006).
- [17] OECD Working Party for Manufactured Nanomaterials (WPMN). "Emission Assessment for Identification of Sources and Release of Airborne Manufactured Nanomaterials in the Workplace: Compilation of Existing Guidance." ENV/JM/MONO(2009)16. Organisation for Economic Co-operation and Development (OECD), Head of Publication Service, OECD, 2 rue André-Pascal, 75775 Paris Cedex 16, France, (2009). <http://www.oecd.org/dataoecd/15/60/43289645.pdf>.
- [18] Brouwer DB, Van Duuren-Stuurman B, Berges M, Jankowska E, Bard D, and Mark D. "From Workplace Air Measurement Results Toward Estimates of Exposure? Development of a Strategy to Assess Exposure to Manufactured Nano-Objects." *Journal of Nanoparticle Research* 11, no. 8 (2009): 1867-81.
- [19] National Institute for Occupational Safety and Health. "Approaches to Safe Nanotechnology - Managing the Health and Safety Concerns Associated With Engineered Nanomaterials." DHHS (NIOSH) Publication No. 2009-125. U. S. Department of Health and Human Services, Centers for Disease Control and Prevention (CDC), (2009). <http://www.cdc.gov/niosh/docs/2009-125/pdfs/2009-125.pdf>.
- [20] Drew R, and Frangos J. *Engineered Nanomaterials: A Review of The Toxicology and Health Hazards*. Safe Work Australia, (2009). ISBN 978 0 642 32921 9.
- [21] Jackson N, Lopata A, Elms T, and Wright P. *Engineered Nanomaterials:*

Evidence on the Effectiveness of Workplace Controls to Prevent Exposure. Safe Work Australia, (2009). ISBN 978-0-642-32884-7.

- [22] Heim M, Mullins BJ, Wild M, Meyer J, and Kasper G. "Filtration Efficiency of Aerosol Particles Below 20 Nanometers." *Aerosol Science and Technology* 39, no. 8 (2005): 782-89.
- [23] National Institute for Occupational Safety and Health. "Documentation of the NIOSH Validation Tests." DHEW publication no. (NIOSH) 77-185. U. S. Department of Health, Education and Welfare, (1977).
- [24] National Institute for Occupational Safety and Health. *Asbestos by TEM, Method 7402, Issue 2*. NIOSH, (1994).
- [25] Li Q, Zhang X, Depaula RF, Zheng L, Zhao Y, Stan L, Holesinger TG, Arendt PN, Peterson DE, and Zhu YT. "Sustained Growth of Ultralong Carbon Nanotube Arrays for Fiber Spinning." *Advanced Materials* 18, no. 23 (2006): 3160-3163.
- [26] Liu K, Sun Y, Chen L, Feng C, Feng X, Jiang K, Zhao Y, and Fan S. "Controlled Growth of Super-Aligned Carbon Nanotube Arrays for Spinning Continuous Unidirectional Sheets With Tunable Physical Properties." *Nano Letters* 8, no. 2 (2008): 700-705.
- [27] Zhang M, Atkinson KR, and Baughman RH. "Multifunctional Carbon Nanotube Yarns by Downsizing an Ancient Technology." *Science* 306, no. 5700 (2004): 1358-61.
- [28] Jiang K, Li Q, and Fan S. "Nanotechnology: Spinning Continuous Carbon Nanotube Yarns." *Nature* 419, no. 6909 (2002): 801.
- [29] Hawkins SC, Poole JM, and Huynh CP. "Catalyst Distribution and Carbon Nanotube Morphology in Multilayer Forests by Mixed Cvd Processes." *Journal of Physical Chemistry C* 113, no. 30 (2009): 12976-82.
- [30] Huynh CP, and Hawkins SC. "Understanding the Synthesis of Directly Spinnable Carbon Nanotube Forests." *Carbon* (Submitted for publication).
- [31] ASTM International. *Standard Practice for Asbestos Detection Limit Based on Counts, D 6620 - 06*. IHS, (2006).
- [32] TSI Incorporated. "Measuring Nanoparticle Exposure." Application Note NSAM-001. TSI Incorporated, 500 Cardigan Road, Shoreview, MN 55126-3996 USA, (2008).
http://www.tsi.com/uploadedFiles/Product_Information/Literature/Application_Notes/NSAM-001appnote.pdf.
- [33] U.S. Environmental Protection Agency. "Test Method 5 - Particulate Matter (PM)." CFR Promulgated Test Methods. Technology Transfer Network, Emission Measurement Center (US EPA). <http://www.epa.gov/ttn/emc/promgate/m-05.pdf>.
- [34] Johnson DR, Methner MM, Kennedy AJ, and Steevens JA. "Potential for

Occupational Exposure to Engineered Carbon-Based Nanomaterials in Environmental Laboratory Studies." *Environmental Health Perspectives* 118, no. 1 (2009): 49-54.

- [35] Maynard A, Ku B, Emery M, Stolzenburg M, and McMurry P. "Measuring Particle Size-Dependent Physicochemical Structure in Airborne Single Walled Carbon Nanotube Agglomerates." *Journal of Nanoparticle Research* 9, no. 1 (2007): 85-92.
- [36] Standards Australia. High Efficiency Particulate Air (HEPA) Filters - Classification, Construction and Performance, AS 4260-1997. Committee ME/80, Air Filters. Standards Australia, 1 The Crescent, Homebush, NSW 2140, Australia, (1997).
- [37] Standards Australia. Respiratory Protective Devices, AS/NZS 1716:1994. Committee SF/10, Standards Australia, 1 The Crescent, Homebush, NSW 2140, Australia, (1994).

Appendix A: Background-“Free” Challenges of Synthetic Carbon Nanotubes

The Hazardous Aerosol Test Duct is equipped with the following provisions:

- An atomiser for the generation of CNT aerosols.
- Sampling tubes for aerosol sampling by real-time detection techniques.
- A sampling cowl for membrane-based sampling.
- Various filter systems for safe use of the instrument where recirculation cannot be implemented.
- Absorber cartridges to strip solvent-vapours from the air stream and ensure reliable operation of the atomisation process.

These features are illustrated in more detail in the following sections.

Aerosol generation

In the deliberate creation of CNT aerosols, the initial emphasis is placed on making sure that objects are created in concentrations that suit the techniques used for their detection. This comes at the expense of ensuring that the structure of airborne CNT is consistent with those released e.g. by pertinent manufacturing processes; addressing this objective is beyond the scope of this study.

Typical properties of CNT manufactured by CSIRO are summarised in Table 2. All CNT manufactured at CSIRO are grown by Chemical Vapour Deposition (CVD), but there are two different methods that are commonly used in conjunction with this technique, as was discussed in Section 3.1.

The creation of a CNT aerosol involves dispersing CNT in 2-propanol and atomising the dispersion to generate small droplets. The 2-propanol component in each droplet evaporates over time into the surrounding gas stream and leaves behind the CNT (or bundle of CNT) as an airborne nano-object.

Containment for synthetic hazardous aerosols and sampling provisions

A sketch of the whole Test Duct for synthetic hazardous aerosols is shown in Figure 19 and a part of the instrument is shown in the photo of Figure 3 in Section 3.5, depicting the Cowl Chamber in the centre. The system is configured as a circulating flow. Main parts of the experimental section are shown at the top, associated support systems (located in the return flow) in the centre and energising plant at the bottom of the sketch.

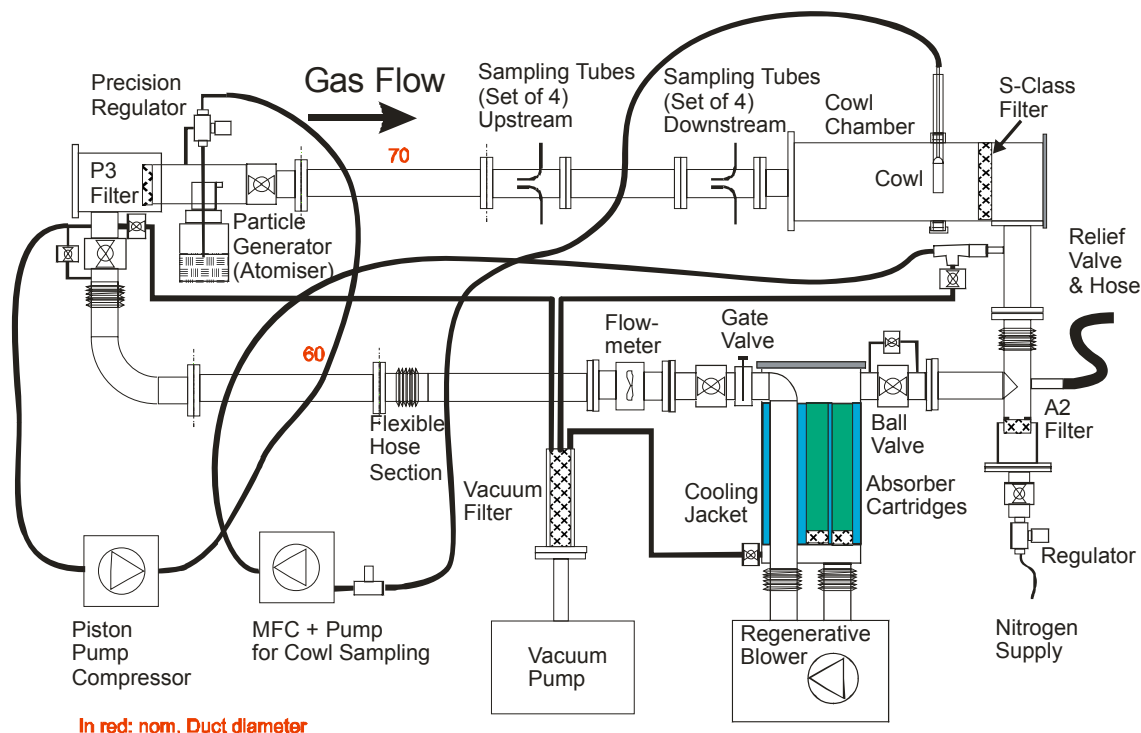


Figure 19: Design sketch of the Hazardous Aerosol Test Duct

The main experimental section of the containment (top of sketch) is a stainless steel pipe of 73 mm inner diameter in which the aerosol objects are travelling within a laminar gas stream. Objects are generated on the upstream end of the pipe by an Atomiser and sampled by two sets of four Sampling Tubes that are oriented at angles of 90° to each other. The tip of each Sampling Tube is bent at a right angle into the airstream that carries the nano-objects from the Atomiser.

After the second set of Sampling Tubes, the diameter of the pipe increases in a step to 199mm to form the Cowl Chamber in which the flow velocity of the airstream is slowed to approximately 13% of the velocity at the inlet. This process is fairly continuous over a distance of approximately 500 mm due to the generation of a taper-shaped return flow, according to predictions from a numerical fluid dynamics model (Figure 20). The airstream returns to a second steady state regime where the return flow ends in the Cowl Chamber. A stainless steel sampling Cowl with a membrane mounted inside is located a short distance away from this point and is used for the sampling of aerosol objects, which remain suspended nearly stationary in the slowly moving flow. These objects are collected on the membrane by the application of negative pressure at the rear of the Cowl mount (Figure 21).

The whole of the experimental section, which extends from the Particle Generator to the Cowl, is contained between fine particle filters at both ends. These filters provide filtration efficiencies $\geq 99.97\%$ (equivalent to a penetration $\leq 3 \cdot 10^{-4}$) for fine solid particles under certain test conditions. This efficiency specification is equivalent to that of Grade 1 HEPA filters used in air-conditioning. In this report, we will be using the term “HEPA” in a wider context than just air-conditioning, which has become popular in filter specific terminology. The term “HEPA” is attributed in this context to any filter medium

that provides a filtration efficiency $\geq 99.97\%$ at a maximum pressure drop of 250 Pa [36] for the specific conditions under which the medium has been tested.

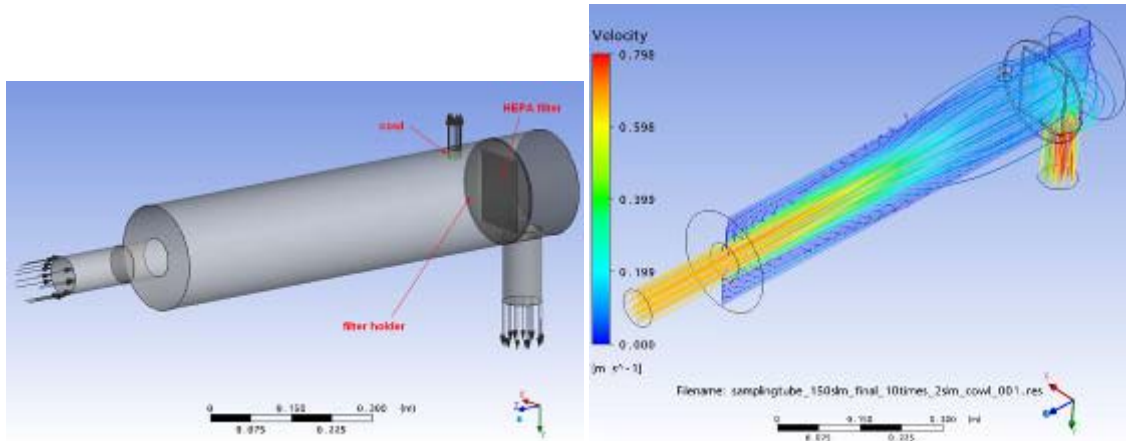


Figure 20: Simulation of airflow streamlines inside the 199 mm cylindrical section of the cowl. The airflow at the inlet is 150 standard litres per minute (SLPM). From this flow 2 SLPM are drawn through the sampling cowl on top of the Cowl Chamber, while the remaining flow is exiting the unit through the outlet behind the HEPA filter

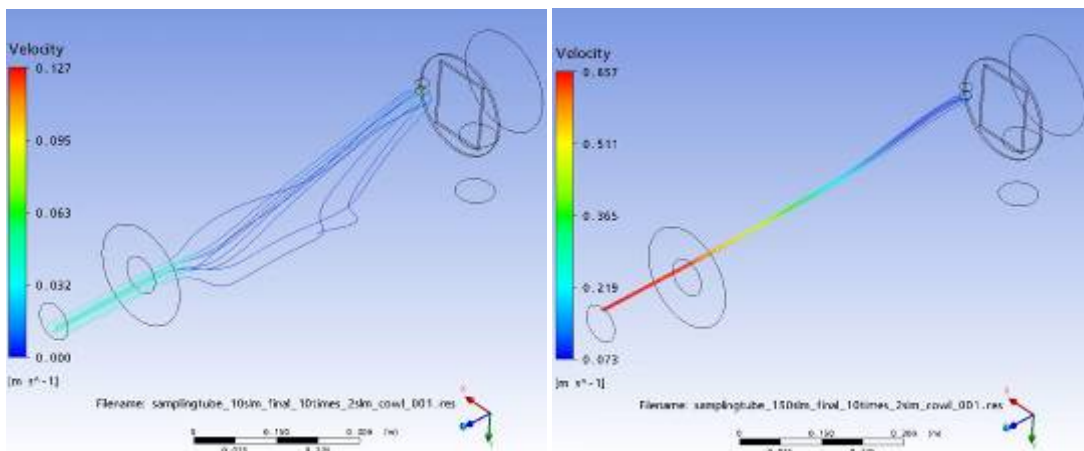


Figure 21: Likely path of dust particles passing through the Cowl Chamber and landing on the membrane inside the cowl for inlet flow rates of 10 SLPM (left) and 150 SLPM (right)

The filter medium that was used in front of the Particle Generator is a P3-rated respirator cartridge, which fulfils a HEPA efficiency rating for flow rates up to 95 litres per minute at the higher initial pressure drop of ≤ 540 Pascal (Table 4.1 in [37]) than the 250 Pascal that are allowed by the HEPA filter standard (definition 1.3.6 in reference [36]). The performance of this medium does not conform to a HEPA filter rating for high flow rates between 95 and 150 litres per minute. But since the air flow is directed

against the source of generated objects, the filter will be exposed to significantly reduced object concentrations and therefore perform as required.

The filter on the inside of the Cowl Chamber is an S-Class filter medium that has been developed for low-allergen vacuum cleaners manufactured by Wertheim (Electrolux). It is unclear if the term "S-Class" refers to an actual standard or a specification which designates a filter medium that conforms to Grade 1 HEPA filter specifications under conditions found in vacuum cleaners. Since vacuum cleaners can deliver flow rates greater than 1000 litres at more than 10 kPa pressure drop, the efficiency and supported flow rate of S-Class filters will be well suited for the purposes of the containment.

The circulating airstream is driven through the interior of the containment by a regenerative side-channel blower. The action of the blower compresses the gas in the containment which is continuously generating heat. The inlet and outlet of the fan blower are therefore contained inside a cooling jacket that has the capacity to extract heat for the purpose of keeping the temperature of the circulating gas in the test instrument constant. The cooling unit is further equipped with three parallel absorber cartridges that provide an interaction length of ca. 0.45 metres. These cartridges can be filled with different absorbents, depending on the dispersant used. We generally use activated charcoal as absorbent for 2-propanol. Experiments have shown that activated charcoal has the capacity of absorbing quantities of 2-propanol of up to 25% of its own weight provided it is activated for 12 hours at 400°C.

The Cowl inside the Cowl Chamber is attached to the end of a stem of the same diameter. The stem is mounted inside a sliding sleeve with 2 O-rings at the top of the cowl chamber. Diametrically opposite is a second sleeve that is normally capped by a screw top lid. During operation of the Cowl, the stem is positioned so that the entrance of the Cowl is located near the central axis of the Cowl Chamber. When aerosol sampling inside the Cowl Chamber has been completed, the entrance of the Cowl is slid into the capped port on the underside of the chamber. From there it is possible to exchange the used Cowl by a new one without having to interrupt a running experiment.

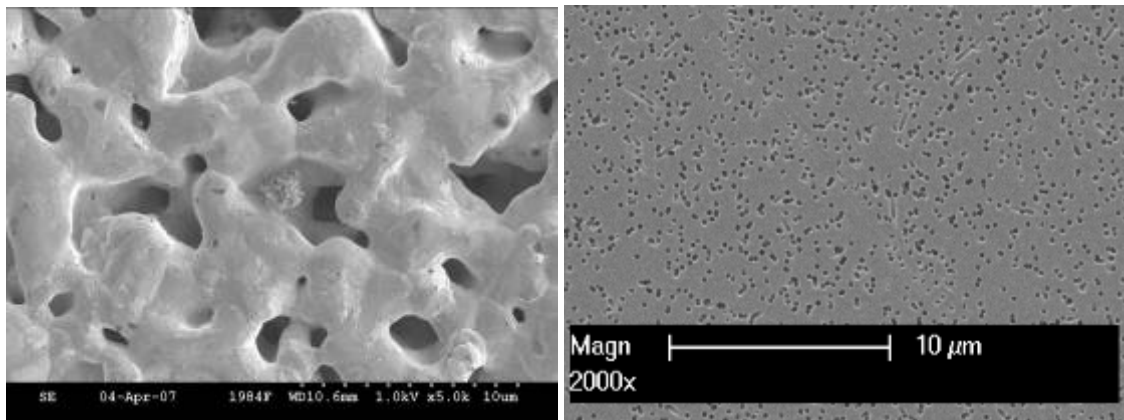
Appendix B: Selection of Membranes

Early experiments that involved air sampling through tortuous path silver membranes (image on the left of Figure 22) highlighted some common issues that have to be considered for the selection of suitable membranes:

- An uneven surface structure makes the detection of objects on the membrane surface by means of optical microscopy or SEM very difficult.
- A significant number of objects are trapped inside the tortuous paths of the membrane and are therefore not visible.

These issues are often resolved by using mixed cellulose ester membranes that are collapsed into a flat, non-porous film after sampling by exposing the membrane to acetone fumes (Table 1).

Track-etched polycarbonate membranes, on the other hand, have smooth surfaces and cylindrical pores, which trap objects on the surface only and provide a featureless background to captured material (left side of Figure 22). However these membranes are non-conductive and severe charging during SEM imaging is generally prohibitive for the use of these membranes without conductive coating.



Left: SEM by Chris Coombs (CSIRO) on Hitachi S4300SE/N. Right: SEM by Kallista Sears (CSIRO) on Philips XL30

Figure 22: SEM image of a tortuous-path Silver Membrane with 0.45 μ m nominal pore size (left) and of a track-etched Polycarbonate membrane with straight cylindrical pores of 200nm diameter (right) at comparable scales

We investigated therefore how the application of a relatively thick gold coating of 70-80nm by means of Argon ion beam sputtering⁸ would affect the pore structure of the membrane (Figure 22). Gas permeability test results conducted on hydrophilic polycarbonate membranes with pore sizes ranging from 30-200nm (set up at the top of Figure 23) clearly indicated that the coating did not change the permeance of the membrane if the gold is applied in this way (Table 3).

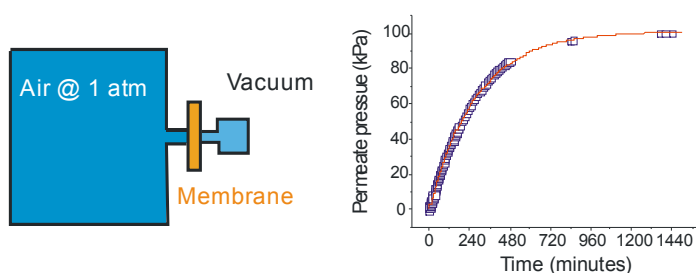
⁸ The head of the sputter coater was a planar argon-ion magnetron sputter source B315 manufactured by Ion Tech Limited (Middlesex, England).

Table 3: Comparison of permeances of polycarbonate membranes in uncoated condition “As is” and after application of a gold coating of 80nm thickness

| Pore Diameter (nm) | Permeance "As is" ($\text{mol m}^{-2} \text{s}^{-1} \text{Pa}^{-1}$) | Permeance Gold Coated ($\text{mol m}^{-2} \text{s}^{-1} \text{Pa}^{-1}$) |
|--------------------|--|--|
| 200 | $1.21 \cdot 10^{-4}$ | $1.13 \cdot 10^{-4}$ |
| 100 | $6.56 \cdot 10^{-5}$ | $6.68 \cdot 10^{-5}$ |
| 80 | $5.11 \cdot 10^{-5}$ | $4.73 \cdot 10^{-5}$ |
| 50 | $2.42 \cdot 10^{-5}$ | $2.55 \cdot 10^{-5}$ |
| 30 | $6.10 \cdot 10^{-6}$ | $6.05 \cdot 10^{-6}$ |

In another characterisation of the membranes, a mass flow controller (MFC) was used to control the gas flow through polycarbonate membranes under the pressure differential that can be produced by a 2-stage piston pump. The application range for different pore size membranes under such conditions was evaluated in the test set up shown at the bottom of Figure 23.

Closed System Test



Constant Flow Test

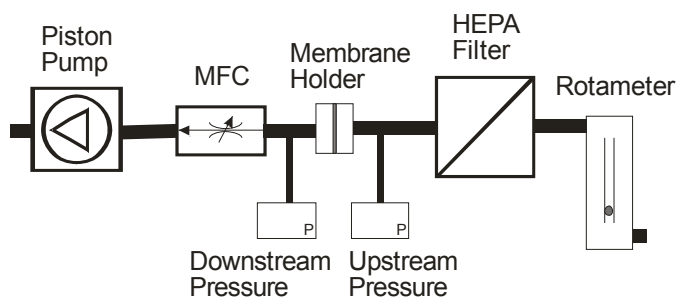


Figure 23: Schematic diagrams of tests used for assessing membrane permeance.

Top: Closed system set up (left) where the membrane under test is exposed to a pressure differential and the change of pressure on the permeate side is monitored over time (right).

Bottom: System where a constant flow is maintained through the membrane (in the membrane holder) by a piston vacuum pump / mass flow controller (MFC) combination. Permeance is characterised by the pressure that is built up across the membrane at the given flow

Readings from the MFC were compared with those of a rotameter at the inlet of the set up and were found to agree within 3%. Another comparison to the calculated flow was made on the basis of the measured pressure differential using permeance values specified by the manufacturer (GE Osmonics). These results are shown in Table 4.

Table 4: Comparison of flow rates set by the Mass Flow Controller (column MFC) to calculated flow rates based on pressure differential and membrane permeances

| MFC (LPM) | Pore Size | | | | |
|--|-----------------------|-----------------------|-----------------------|-----------------------|-----------------------|
| | 200nm | 100nm | 80nm | 50nm | 30nm |
| 1.00 | 0.82 | 0.89 | 0.73 | 0.82 | |
| 2.00 | 1.58 | 1.66 | 1.43 | | |
| 3.00 | 2.35 | 2.49 | | | |
| 4.00 | 3.20 | 3.40 | | | |
| 5.00 | 4.06 | | | | |
| Limit | | 3.40 | 1.98 | 1.11 | 0.25 |
| MFC @ Limit | | 4.00 | 2.75 | 1.37 | 0.37 |
| Permeance (mol m ⁻² s ⁻¹ Pa ⁻¹) | 1.98 10 ⁻⁴ | 9.88 10 ⁻⁵ | 4.94 10 ⁻⁵ | 2.44 10 ⁻⁵ | 4.94 10 ⁻⁶ |

Measurements from the MFC and the rotameter were in good agreement, although calculated values were generally lower. We believe that this is due to a systematic error because absolute deviations are very similar irrespective of pore size. This is most likely due to the test set up, because the fittings used provide changes in pipe diameter and the pressure taps were thicker than the ideal. As a result, the values obtained from MFC and rotameter are considered to be more reliable.

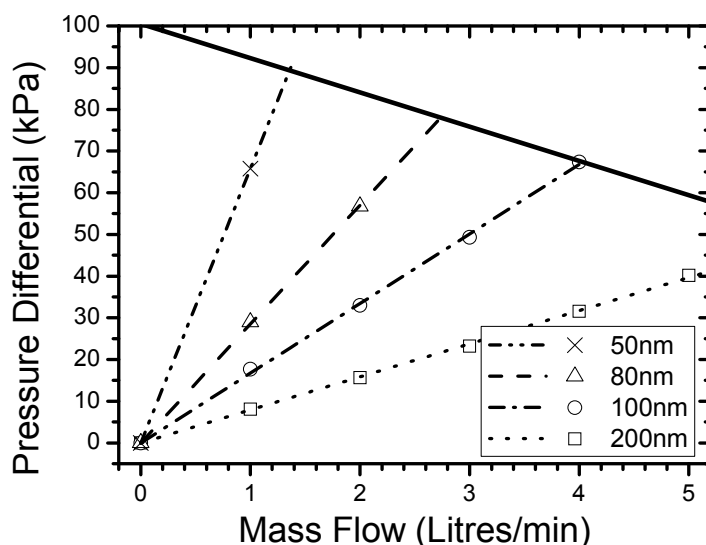
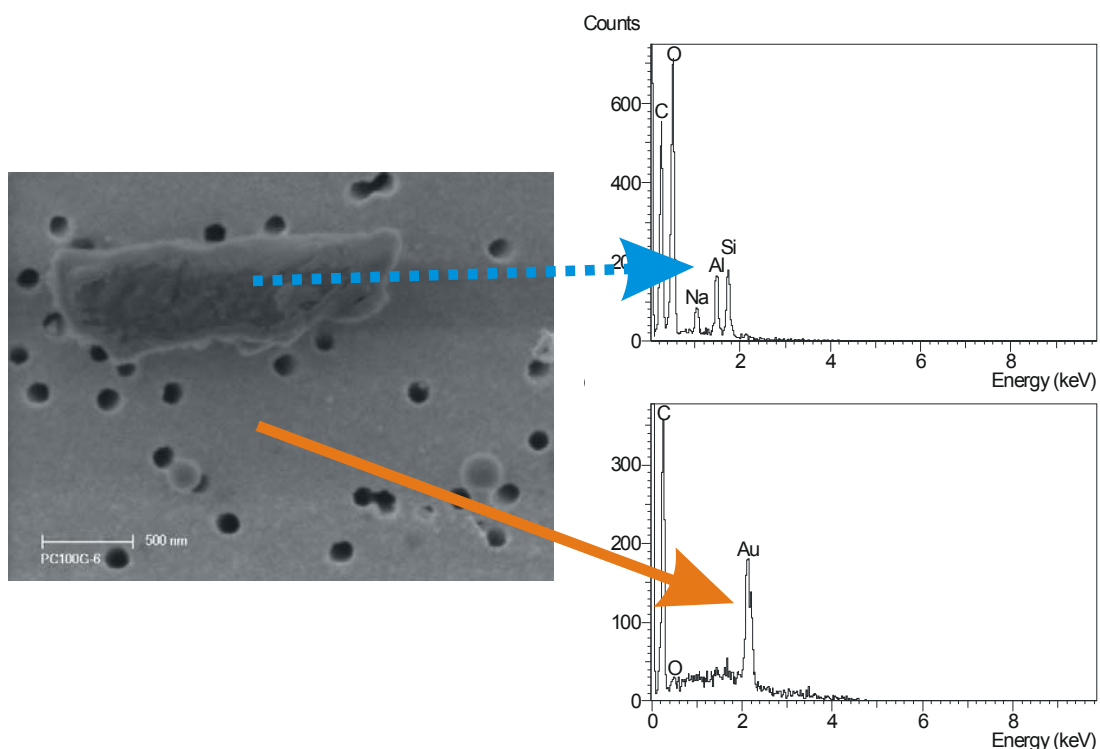


Figure 24: Pressure differential required across polycarbonate membranes of different pore sizes (see legend) to obtain a certain mass flow rate. These values apply for an Aalborg MFC of 5 litres per minute maximum flow

The constant flow test set up of Figure 23 was also useful for determining the operating range for different membrane pore sizes. Figure 24 shows measured pressure differentials for different membrane pore sizes as a function of flow rate. A practical performance limit is indicated by the solid line at the top of the figure, which applies when an Aalborg mass flow controller with five litres per minute maximum flow is used towards ambient pressure.

It is also necessary to take into account that polycarbonate membranes with finer pores generally have higher pore densities. Actual pressure dependencies may therefore vary if membranes from other suppliers are used.

Using polycarbonate membranes with a relatively thick gold coating has the added advantage that the polycarbonate signature of the membrane is largely shaded from Energy Dispersive X-Ray Spectroscopy (EDXS) so that the membrane behaves like a metallic membrane rather than an organic one. This principle was demonstrated for a relatively large fragment collected on one of the gold-coated polycarbonate membranes and identified from the EDXS scan shown in Figure 25 to be inorganic in nature (oxides O of sodium Na, aluminium Al and silicon Si). The lower EDXS scan shows the signature of the gold-coated polycarbonate membrane, which exhibits a very clear gold peak (Au), while all other features appear heavily suppressed. This technique is thus very useful for distinguishing fragments of CNT yarns from those of mineral fibres.



SEM / EDXS by John Ward (CSIRO) on Philips XL30

Figure 25: Identification of the inorganic nature of a coarse fibrous fragment by Energy Dispersive X-Ray Spectroscopy (EDXS)

Appendix C: Reference Membranes

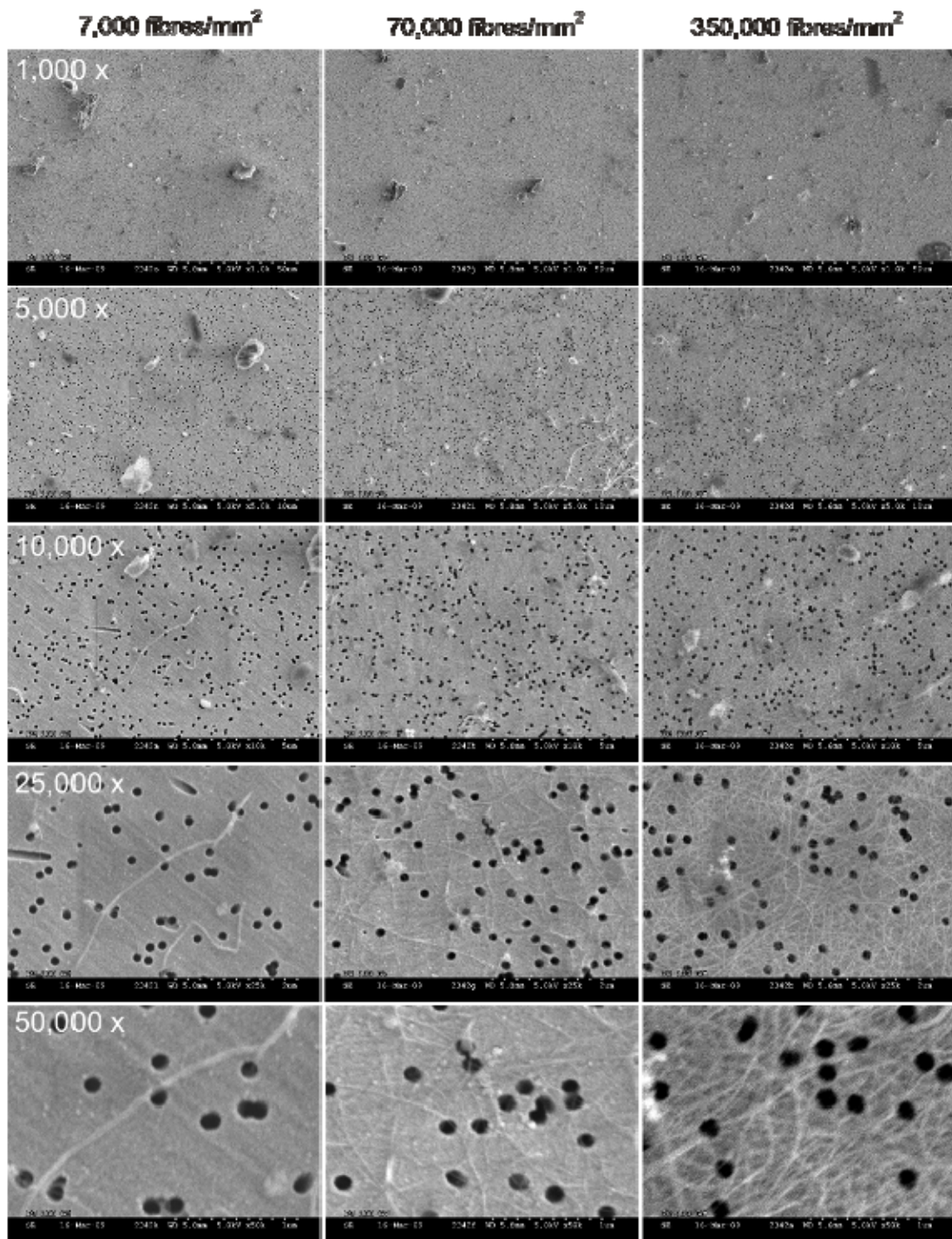
In the lead up to membrane-based sampling experiments it is necessary to work out suitable air sampling rates that allow an investigation be conducted within a reasonable time frame. It is important to have some preliminary knowledge of what the surface of the membrane should look like for a given concentration of particles in the air. This issue can be addressed by creating reference membranes with known estimates for the number concentration of CNT deposited on the membrane surface, which would be the result from drawing a certain volume of air with the given particle concentration through the membrane.

The amount by weight of CNT to be applied to the reference membranes was calculated assuming that all CNT had the same length, as determined from the height of the CNT forest. The required amount of CNT was weighted out on a balance, dispersed in 2-propanol and applied by drawing the dispersion through the membrane using a fritted funnel as a support.

For example, assuming we have a concentration of 1 fibre/ml and a sampling volume of 300 litres the total number of CNT fibres is $3 \cdot 10^5$, and these are spread over a surface area of 380mm^2 (for a membrane with an active area of 22mm diameter, as given by the typical opening of a sealing ring). This means that we expect to find on average a concentration of 790 fibres/ mm^2 on the membrane surface and this value will scale linearly with the concentration of fibres in the air.

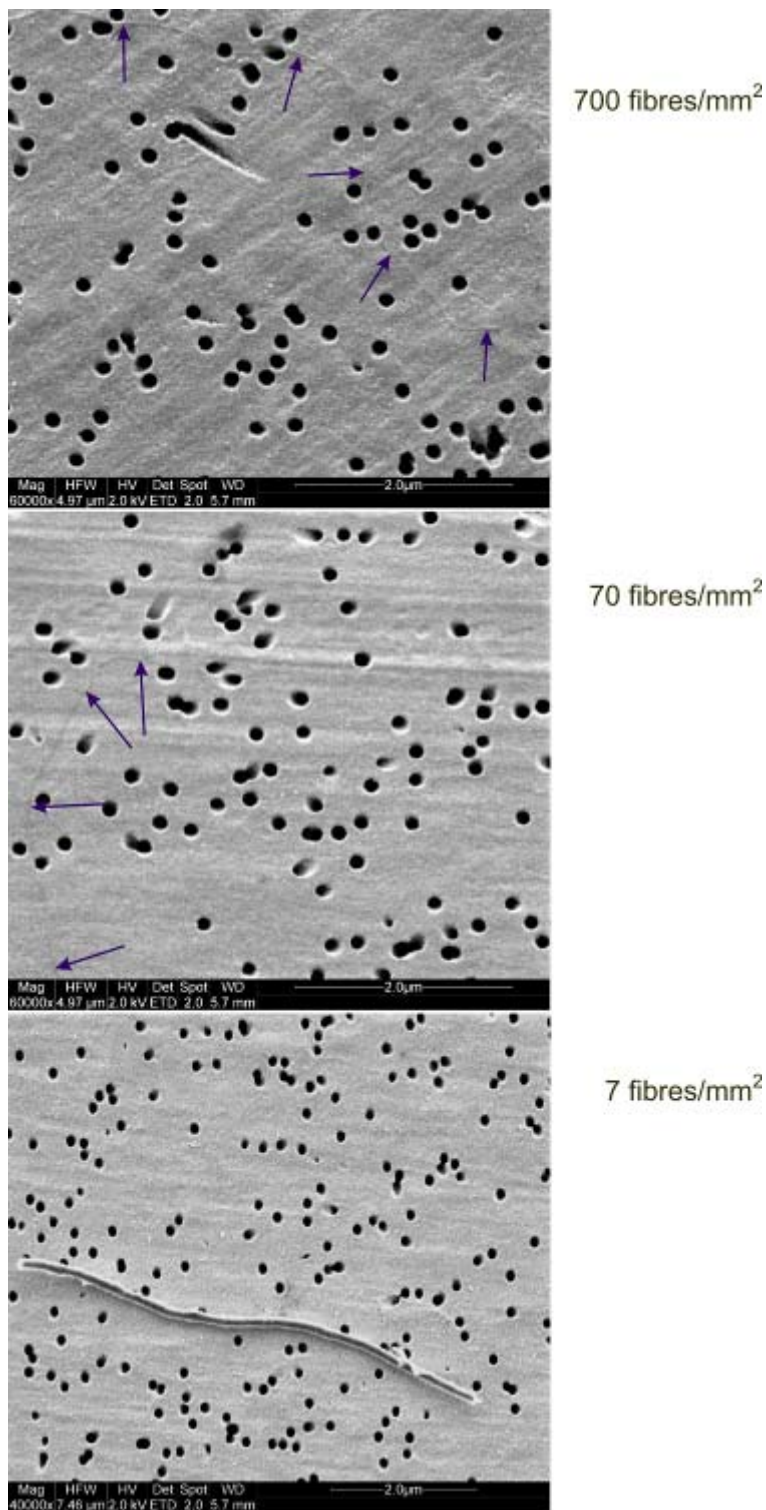
To calculate the required mass of CNT that needs to be dispersed in 2-propanol to obtain a total fibre count of $3 \cdot 10^5$ CNT fibres, we assumed that all CNT would be 200 micrometres long and have a diameter of 10nm. The average mass density of a single CNT was approximated by taking the density of graphite (2.1g/cm^3) and by subtracting the hollow interior from the overall volume of the CNT. This gives a density of approximately 1.7g/cm^3 and a weight of 27 femtograms (10^{-15}g) per CNT. A quantity of 0.6 mg, which is equivalent to $2.2 \cdot 10^{10}$ CNT fibres, was dispersed by ultrasonication in 500ml of 2-propanol and diluted in steps starting from $1.1 \cdot 10^8$ fibres and $2.2 \cdot 10^7$ fibres down to $2.2 \cdot 10^3$ fibres. Each CNT dispersion was filtered through a 25mm polycarbonate membrane of 100nm pore size. The membrane was mounted on a blanking film of 47mm diameter that matched the diameter of the fritted funnel. Dispersed CNT were drawn through a circular opening of 20mm diameter in the centre of the blanking film by application of negative pressure. The resulting fibre concentrations deposited on the membranes were $3.5 \cdot 10^5$ fibres/ mm^2 , $7.0 \cdot 10^4$ fibres/ mm^2 , $7.0 \cdot 10^3$ fibres/ mm^2 , $7.0 \cdot 10^2$ fibres/ mm^2 , $7.0 \cdot 10^1$ fibres/ mm^2 and $7.0 \cdot 10^0$ fibres/ mm^2 . As derived above, $7.0 \cdot 10^2$ fibres/ mm^2 corresponds to a concentration of approximately 1 fibre/ml in air.

These membranes were subsequently imaged on an SEM, which resulted in the images of Figure 26 and Figure 27. A concentration of $1.1 \cdot 10^8$ fibres in a sampling volume of 300 litres, which is equivalent to 367 fibres/ml, formed a whole web of CNT on the membrane and it was impossible to establish an accurate count of fibres in this instance. At the lower end, corresponding to a concentration of $2.2 \cdot 10^3$ fibres in 300 litres of air (or 0.007 fibres/ml), we were unable to find any spinnable CNT.



SEMs by Colin Veitch (CSIRO) on Hitachi S4300SE/N

Figure 26: Spinnable Carbon Nanotubes applied to gold-coated polycarbonate membranes with 100nm pore size from a 2-propanol dispersion. SEM magnification is increased from top to bottom (indicated in the top left corner), while the nominal application level (i.e. assuming all CNT are 200 µm long) is increased between columns: 7,000 fibres/mm² (left), 70,000 fibres/mm² (centre) and 350,000 fibres/mm² (right)



SEMs by Roger Curtain (Bio21) and Jurg Schutz (CSIRO), imaged at the Bio21 Institute in Melbourne on FEI Quanta 200F

Figure 27: Spinnable Carbon Nanotubes applied to gold-coated polycarbonate membranes with 100nm pore size from a 2-propanol dispersion. Nominal fibre concentrations are indicated on the right. The location of the single spinnable CNT that was found in the upper 2 images is marked by arrows. The fibre in the image at the bottom exceeds the diameter of spinnable CNT

The only fibrous structure found at the lowest concentration is shown in Figure 27. This fibre was too coarse to be a spinnable CNT and it seems plausible that the contaminant was introduced via the glassware (either a CNT grown by Continuous Catalyst Injection (CCI) or a mineral fibre; see Section 3.1 for details).

Appendix D: Analysis of Membrane Samples by Electron Microscopy

Asbestos standards (Table 1) provide an excellent description of the options available to address these points. It is however advisable to make minor adjustments since spinnable CNT are generally significantly thinner than asbestos fibres and consist of pure carbon. We decided to use the SEM Method described in ISO Standard 14966:2002(E) [4] for this work because the preparative steps prior to imaging were less onerous than those of the TEM methods.

We had also made up reference membranes that had been coated with controlled amounts of spinnable CNT (see Appendix C) to give us an idea of what we were looking for and demonstrated that SEM was capable of detecting individual CNT. It needs to be noted though, that SEM imaging is clearly reaching its limits in terms of resolution and cannot determine if a fibre structure is a single CNT or a small bundle of several CNT (Figure 28). One possible solution to this problem would be to image the same sample by means of Scanning Probe Microscopy (SPM), which can reach the resolution required for assessing the structure of individual CNT or CNT fibre bundles.

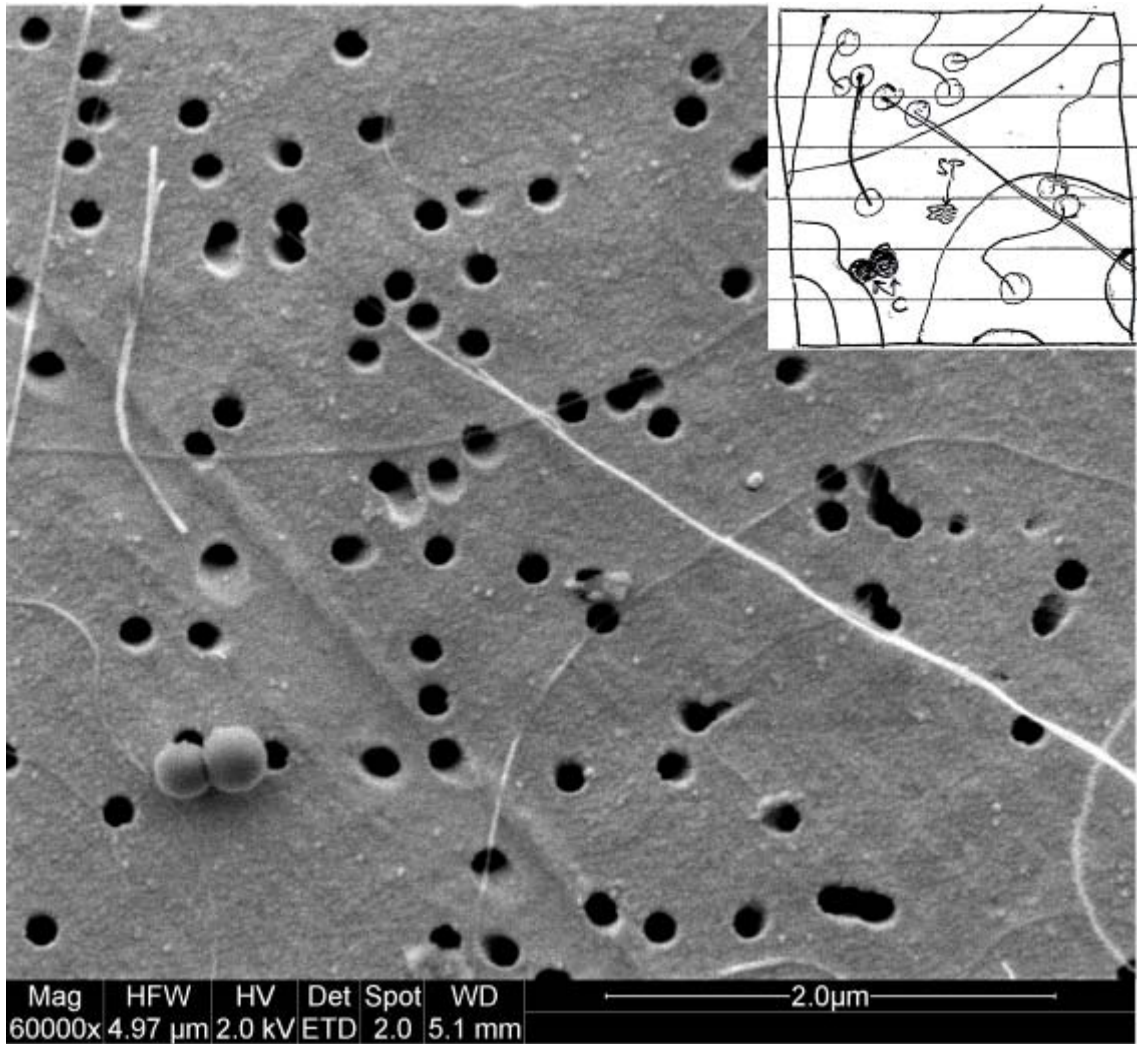
ISO Standard 14966:2002(E) also suggests to remove organic contamination picked up during sampling by ashing with oxygen plasma. Since CNT are decomposed by oxygen-containing plasmas it is not possible to adopt this practice for CNT aerosols. However, in the specific situation of the CNT Yarn Spinning Laboratory we found that there was no need for this procedure because particle and general contamination levels were very low and particle background was not a problem. The gold-coating was still applied to the membrane because, although the membranes could be imaged without the need to apply a conductive coating after sampling, it suppressed the organic nature of the polycarbonate membrane for use with Energy Dispersive X-Ray Spectroscopy (EDXS).

In determining the size of the visibility field, we imaged the CNT coated polycarbonate membranes to find the lowest magnification required to image low concentrations of the very finest fibre structures. We conducted investigations on three different SEMs (Hitachi S4300SE/N, Philips XL30, FEI Quanta 200F) and found that the lowest magnification was in the vicinity of 60,000x. However, this value may not be universally applicable to all SEMs. It was found that low acceleration voltages of 2kV or 5kV generally produced better contrast in terms of being able to distinguish CNT structures from the characteristic signature of the membrane. All SEM images were obtained from secondary electrons.

From the range of counting rules commonly used in assessing dust deposits from asbestos sampling, we decided to adopt for spinnable CNT the counting of fibre ends. However, because the ends of these types of CNT are hard to identify clearly, it appeared to be sensible to count each end as half a fibre, irrespective of how the fibre end was oriented in the viewing field. A summary of counted structures from a polycarbonate membrane that was coated with a nominal concentration of 7000 fibres/mm² according to calculations made in Section 3.3.1 is shown in Table 5. Even

though spinnable CNT are extremely long in comparison to their diameter, it was found that the majority of structures identified were fibres that exhibited one fibre end in the selected view field, not fibres passing through the view field without showing any ends.

By carrying out the statistics it appears that each CNT fibre was on average broken into 50 pieces, which is most probably due to extensive ultrasonication that was needed to keep the CNT suspended in solution as individual fibres or small bundles. This means that the effective fibre count of membrane samples shown in Figure 26 and Figure 27 was approximately 50 times the nominal value.



SEM by Jurg Schutz (CSIRO) imaged at the Bio21 Institute in Melbourne on FEI Quanta 200F. Sketch of objects identified (CNT ends circled)

Figure 28: SEM image of frame _005 from Table 5 with a hand-drawn sketch that was used to apply the counting rules (inset)

Despite all the challenges, e.g. with the resolution of CNT ends using SEM, what made the task of counting CNT fibres relatively easy and reliable was the fact that these structures differ significantly in fineness and character from typical contaminants that are being picked up during preparation of the membranes or during sampling. Further,

even if the exact position of a CNT end cannot be determined, it is generally sufficient to say that a certain fibre is entering the viewing field but has no continuation in order to decide in favour of a single fibre end.

Table 5: Summary of objects counted on 13 randomly selected view fields from a gold-coated polycarbonate membrane of 100nm pore size with a nominal CNT fibre density of 7000 fibres/mm² (see Section 3.3.1 for preparation details)

| File | Ends (CPD) | CFN | CFE | C2E | Cells | SPA | LPA | SFO | LFO | CPP |
|------|------------|-----|-----|-----|-------|-----|-----|-----|-----|-----|
| Sum | 197 | 52 | 107 | 45 | 10 | 28 | 2 | 12 | 8 | 7 |
| _003 | 12 | 3 | 6 | 3 | 1 | 3 | 1 | | | |
| _004 | 17 | 5 | 9 | 4 | | 1 | | 2 | 2 | |
| _005 | 11 | 7 | 5 | 3 | 2 | 1 | | | | |
| _006 | 15 | 3 | 9 | 3 | 1 | 3 | | | | 1 |
| _007 | 14 | 2 | 8 | 3 | | 2 | | | | 3 |
| _008 | 11 | 4 | 9 | 1 | | 2 | | 2 | 1 | |
| _009 | 24 | 0 | 8 | 8 | 1 | 4 | | | 3 | 1 |
| _010 | 17 | 6 | 9 | 4 | | 1 | | 1 | | |
| _011 | 9 | 6 | 9 | 0 | 2 | 2 | | | | 1 |
| _012 | 19 | 6 | 9 | 5 | | 3 | | 5 | 2 | |
| _013 | 16 | 3 | 12 | 2 | 1 | 2 | | | | 1 |
| _014 | 18 | 2 | 8 | 5 | | 4 | | | | |
| _015 | 14 | 5 | 6 | 4 | 2 | | 1 | 2 | | |

Abbreviations: CFN: Spinnable CNT crossing the viewing frame without exhibiting an end; CFE: CPD CNT exhibiting one fibre end; C2E: Spinnable CNT exhibiting both ends; Cells: Structure that looks like a living cell (bacterium, spore, etc.); SPA/LPA: small/large solid particles and agglomerates; SFO/LFO: small/large fibrous object; CPP: CNT protruding out of a membrane pore.

Summary of findings from counting objects that consist of fine, spinnable CNT on gold coated polycarbonate membranes:

- Spinnable CNT should be imaged at magnification 60,000 to ensure that individual CNT or thin CNT bundles are not missed.
- Spinnable CNT are relatively easy to distinguish from particle background because they clearly differ in shape and size from typical background objects. CCI CNT, on the other hand, are hard to distinguish from mineral fibres that occur quite regularly in natural particle background.
- Spinnable CNT fibres are broken 50 times on average, probably due to the use of ultrasonication.
- While it is not possible to distinguish between individual CNT and small bundles of CNT using an SEM, it would be possible to overcome this problem by inspecting the sample by Scanning Probe Microscopy (SPM).

Appendix E: Upper Detection Limits

If the particle concentration in a working environment is low it may happen that no particles are found on the membrane during membrane-based sampling. In this situation it is possible to quote a detection limit representing an upper limit to the true particle concentration in the air, rather than specifying a structure concentration.

ASTM Standard D 6620-06 [31] describes a statistical approach for this situation. It is based on an alternative model that describes the distribution of objects of interest and a null model that describes background particles that could be mistaken for the object of interest. These distributions are described by partially overlapping Poisson distributions with population means λ_a and λ_0 , respectively. This means that any object of interest that is found on the membrane surface could potentially belong to the background that was present on the membrane prior to sampling (null model) or could have been picked up during the actual air sampling experiment (alternative model). To decide in favour of the alternative model, the number of structures counted (structure count) must be greater than the decision value, x_0 .

The decision value x_0 is an integer that denotes a certain point on the abscissa of the Poisson distribution for the null model, for which the probability that a structure count from this population will exceed x_0 is smaller than or equal to the so-called significance level, α . It is obtained by adding up probabilities from infinity towards zero until the significance level is reached or exceeded. The value of x_0 is determined from a number of blanks, which are membranes that have not been subject to air sampling but have otherwise been treated in exactly the same way. Details are provided in Section 6.4.2 and Appendix X1 of the standard [31].

Reporting of structure count results from a membrane subjected to air sampling (as represented by the alternative model) depends on a number of factors and is carried out as follows:

- If the mean structure count X is greater than the decision value, x_0 , the result is multiplied by the sensitivity S , which is a factor that converts structure count to structure concentration, and reported as an estimate for the measured structure concentration in fibres/cm³.
- If the mean structure count X is less than or equal to the decision value, x_0 , the result is reported as “below detection” because the measured level cannot be distinguished from the background. The detection limit (DL) in fibres/cm³ is calculated as $S \cdot \mu_0$, where μ_0 is a factor that takes into account the probability that the result was attributed to the background (null model) when the structures have in fact been picked up during sampling (alternative model). The magnitude of this factor depends on the chosen probability to exclude this error, the so-called power, n , and on the decision value x_0 . Pertinent values are listed in Tables 1 and 2 of ASTM Standard D 6620-06 for different values of significance level α and power n .

From the air sampling experiment conducted on 26 February 2009, we have the following information:

| | |
|----------------------------------|---|
| Membrane area: | diameter = 22mm; area A = 380mm ² |
| No. of SEM fields viewed: | 20 |
| SEM view area: | width = 4.93 μm; X/Y-ratio = 0.68; view area = 16.5·10 ⁻⁶ mm ² |
| Sampled air volume: | V = 174·10 ³ cm ³ |
| Structure count: | 0 (spinnable CNT) |

A number of considerations need to be made to calculate a detection limit:

- From the number of SEM frames investigated (blanks and samples) we estimate that the applicable decision value is $x_0 = 0$; the significance level has no bearing in this situation because the chosen technique provides no information on the population of background structures.
- The resulting sensitivity S is $(380/20/16.5 \cdot 10^{-6}/174 \cdot 10^3) = 6.62 \text{ cm}^{-3}$.
- Since structure count and decision value are both zero, the result is reported as "below detection".
- If we choose a power of 0.95 the resulting value of μ_0 is 3.00 according to Table 1 or Table 2 of the ASTM Standard D 6620-06.

To calculate the detection limit (DL) we multiply the sensitivity S with μ_0 .

In conclusion we report the structure count in the CNT Yarn Spinning Laboratory as "below detection" with a detection limit of 19.9 fibres/cm³.

Appendix F: Assessment Of The Laboratory Air Environment

Background

The Carbon Nanotube Yarn Spinning Laboratory in Belmont was monitored on 26 February 2009 over a one day period using:

- TSI Sidepak Aerosol sampler, fitted with a PM_{2.5} impactor and 0.2m of Tygon tubing. Samples in µg/m³ were taken every 10 seconds over a period of 30 minutes.
- TSI Condensation Particle Counter 3007 fitted with 0.1m of conductive tubing. Samples in particles/cm³ (p/cc) were taken at one minute intervals over a sample period of 30 minutes.
- TSI Aerotrak 9000 fitted with 0.8m of conductive tubing. Alveolar (A) mode or Tracheobronchial (TB) mode samples in µm²/cc were taken every 10 seconds over a period or 30 minutes.

Monitoring was conducted at three locations:

- Outdoors, adjacent to the laboratory area via an open window.
- At a height of 1.2m above the floor in the CNT laboratory while the spinning was inactive, at a location sited approximately 5m from the yarn spinning rig.
- At the spinning rig, with sampling tubes at approximately 0.2m directly above the spindle.

Sequential measurements were made outdoors to determine trends in particle levels that would eventually influence particle levels indoors.

Results

Results are summarised in Table 6. Note that the measurements are presented in the order they were collected and activities within the lab are noted by comment.

The initial measurement by the Aerotrak(A) was higher within the lab than outdoors but was at approximately the same level as outdoors for the first spinning process sample. The duplicate spinning process sample was much higher than the first, and similar to the outdoor sample. The subsequent outdoor air sample showed the Aerotrak(A) level had increased significantly over the day. Bureau of Meteorology records (Figure 29) showed that there was a rapid wind-shift from North to South at approximately the time of the spinning samples. It is considered that this caused the rise in Aerotrak(A) levels in the duplicate spinning sample. Note that the CPC measurements exhibited similar changes as the Aerotrak(A) measurements, while the PM_{2.5} measurements reduced to near zero during the day.

During each 30 minute sampling, the operator usually stopped the spinner for three to four minutes while a new forest was installed. No step change was observed in the Aerotrak(A) or CPC responses with such activity (Figure 30).

Table 6: Aerosol sampling results (average concentrations)

| Sample no. | Location | $\mu\text{m}^2/\text{cc}$ | | CPC 3007 p/cc | PM _{2.5} $\mu\text{g}/\text{m}^3$ | Comments |
|------------|--------------|---------------------------|---------|------------------|---|---------------------------|
| | | Aero A | Aero TB | | | |
| 1 | Inactive Lab | 15.7 | - | 6,600 | 6 | No staff in lab (10:50am) |
| 2 | Outdoor | 8.6 | - | 3,200 | 2 | Warm, mod. N wind, midday |
| 3 | Inactive Lab | - | 1.3 | 2,000 | 1 | - |
| 4 | Outdoor | 4.5 | - | 1,900 | 0 | 1pm |
| 5 | CNT Spin | 5.8 | - | 4,900 | 0 | 2:00-2:30pm |
| 6 | CNT Spin | 15.7 | - | 8,800 | 0 | 2:30-3:00pm |
| 7 | CNT Spin | - | 4.3 | 9,200 | 0 | 3:00-3:30pm |
| 8 | Outdoor | 29.0 | - | 16,000 | 0 | 3:30pm |
| 9 | Outdoor | - | 5.8 | 11,000 | 0 | |

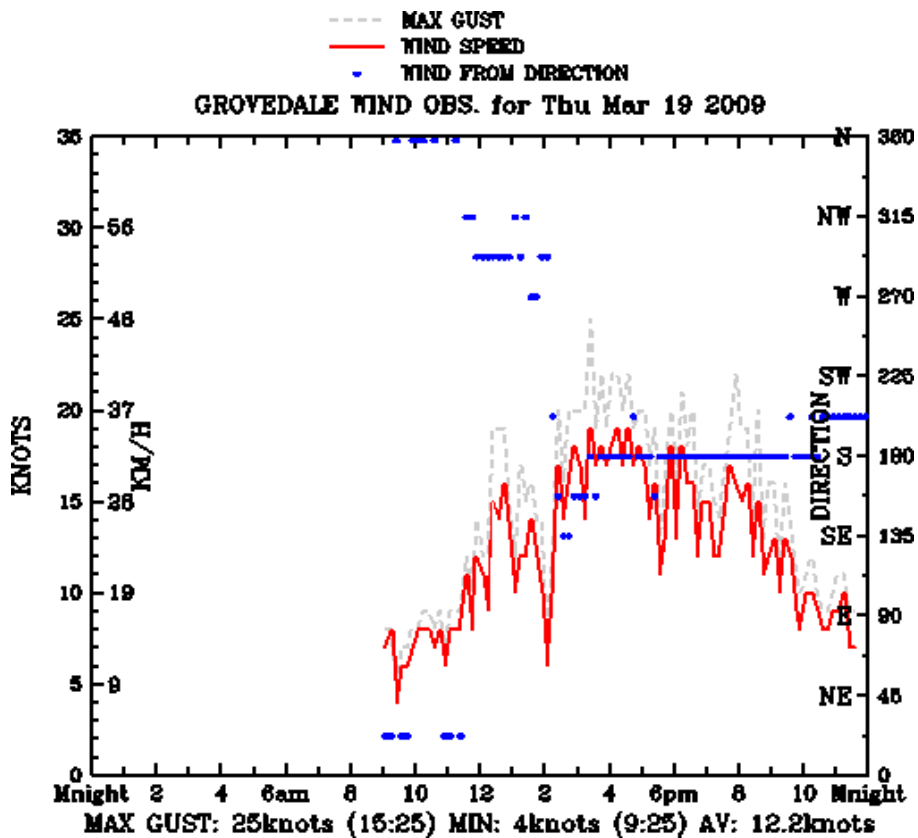


Figure 29: Wind pattern in the vicinity of Belmont (Grovedale) on day of sampling

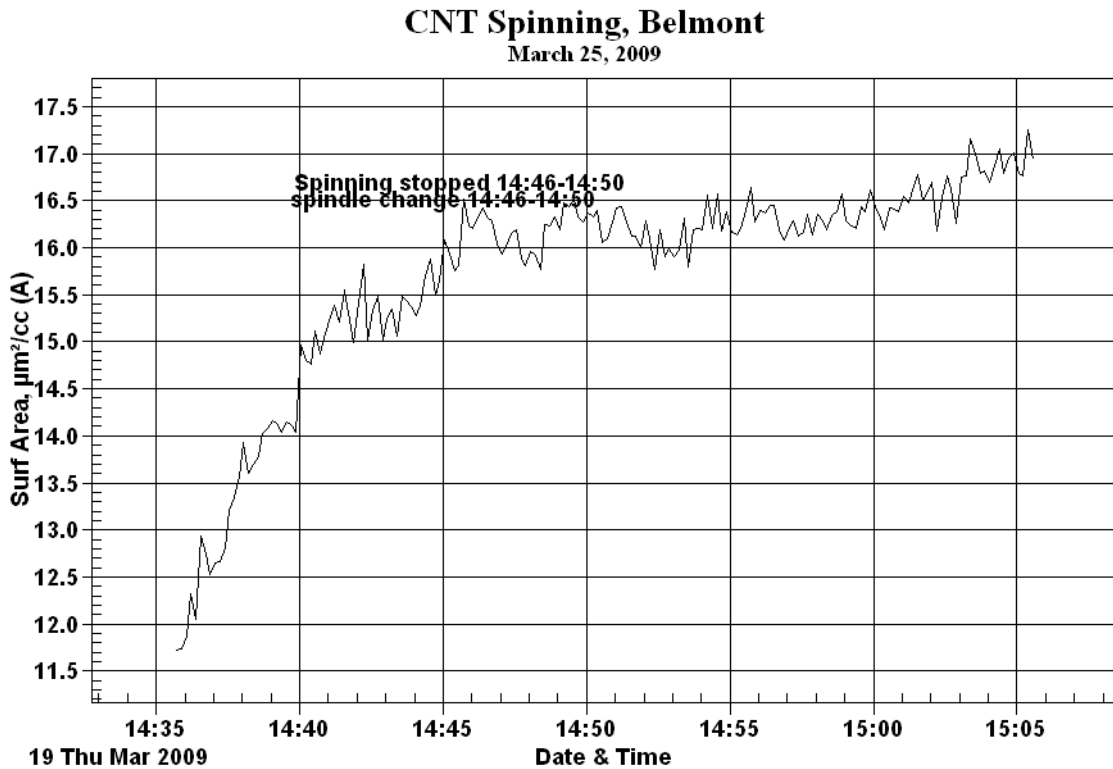


Figure 30: Aerotrak (A) sampling at the spinning process (interruption of time process noted in the plot)

Summary

Generally, none of the measurements exhibited increases that were considered to be associated with the CNT spinning activities. A large increase in particle levels was observed when collecting a second spinning sample compared with a prior sample, but this was considered to result from a large increase in outdoor particle levels, probably associated with a wind-shift from northerly to southerly at that time. This occurrence clearly illustrates the impact, which changes of particle concentrations in the surrounding environment can have on measurements in the laboratory. Observations of start-stop operation during the spinning process showed no related change in particle levels at the spinner.